

# Reference-free XRF and GIXRF analysis

Burkhard Beckhoff

Physikalisch-Technische Bundesanstalt  
Abbestraße 2-12, 10587 Berlin, Germany

- **analytical challenges for nanotechnologies**
- **reference-free x-ray spectrometry**
- **surface contamination and nanolayer characterization**
- **depth profiling at grazing incidence**
- **chemical speciation at buried interfaces**
- **towards in-situ speciation of bulk-type films**
- **high-resolution spectrometry**

# Analytical challenges for nanotechnologies

---

- dozens of **new nanoscaled materials** appear every month
- **technology R&D cycles** for new materials down to 4 months
- **need for correlation** of material properties with functionality
- **requirements** on sensitivity, selectivity and information depth
- most **analytical methodologies** rely on **reference materials** or calibration standards but there are only few at the nanoscale
- usage of **calibrated instrumentation** and knowledge on atomic data enables **reference-free techniques** such as SR based XRS

# Challenges for nanotechnologies – nano-scaled reference materials



X-ray and IR spectrometry

## Nanoscaled Reference Materials ( in line with ISO/TC 229 Nanotechnologies )

*,Reference materials are the key to guaranteeing reliability and correctness for results of chemical analyses and technical measurements.‘*

### Categories:

- flatness
- film thickness
- single step , periodic step, step grating
- lateral X-Y-axis, 1-dim
- lateral X-Y-axis, +2-dim,
- critical dimensions
- 3-dimensional
- nanoobjects/nanoparticles/nanomaterial
- nanocrystallite materials
- porosity
- depth profiling resolution

Every month several tens new nanoscaled materials appear.

The number of nanoscaled reference materials is considerably lower.

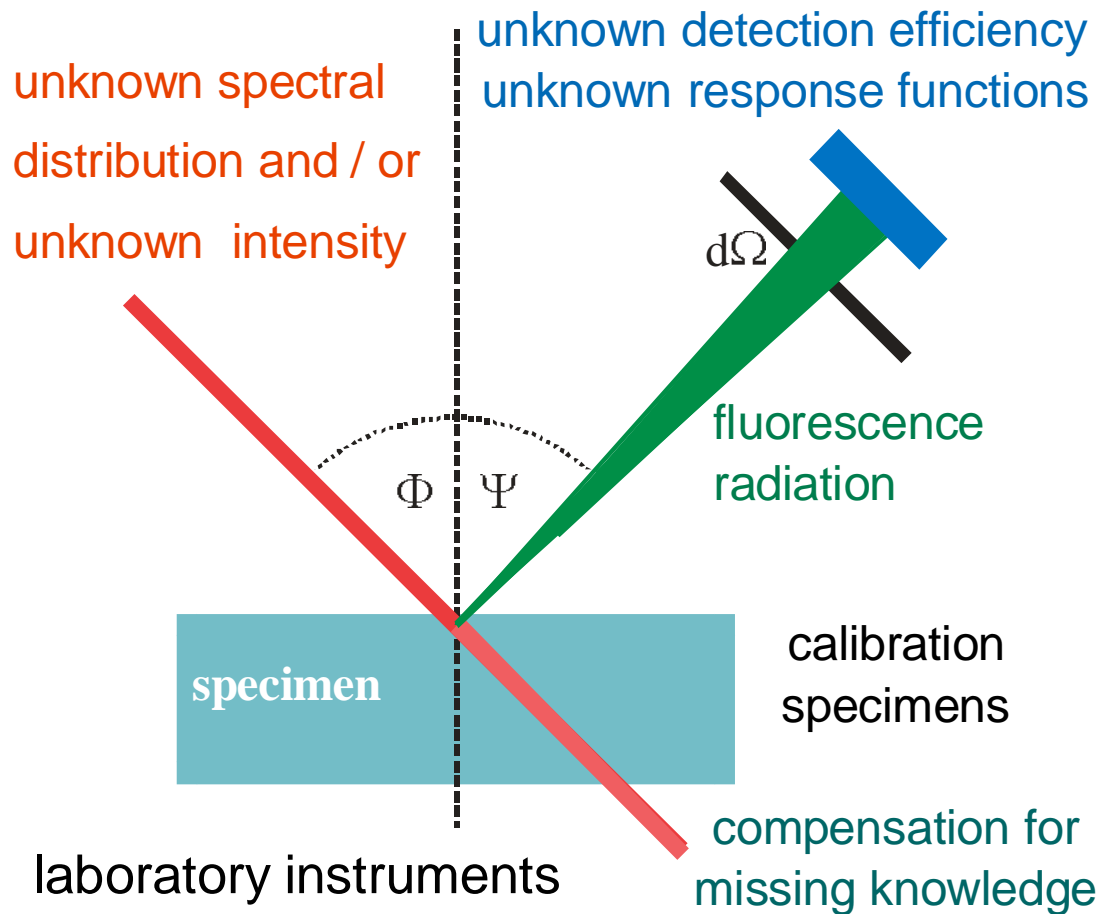
Reference-free / first principles based methodologies can address this increasing gap.

[www.nano-refmat.bam.de/en/](http://www.nano-refmat.bam.de/en/)

# X-ray spectrometry methodologies:

## reference-based versus reference-free approaches

reference material related technique  
based on well known calibration  
specimens or reference materials



# X-ray spectrometry methodologies:

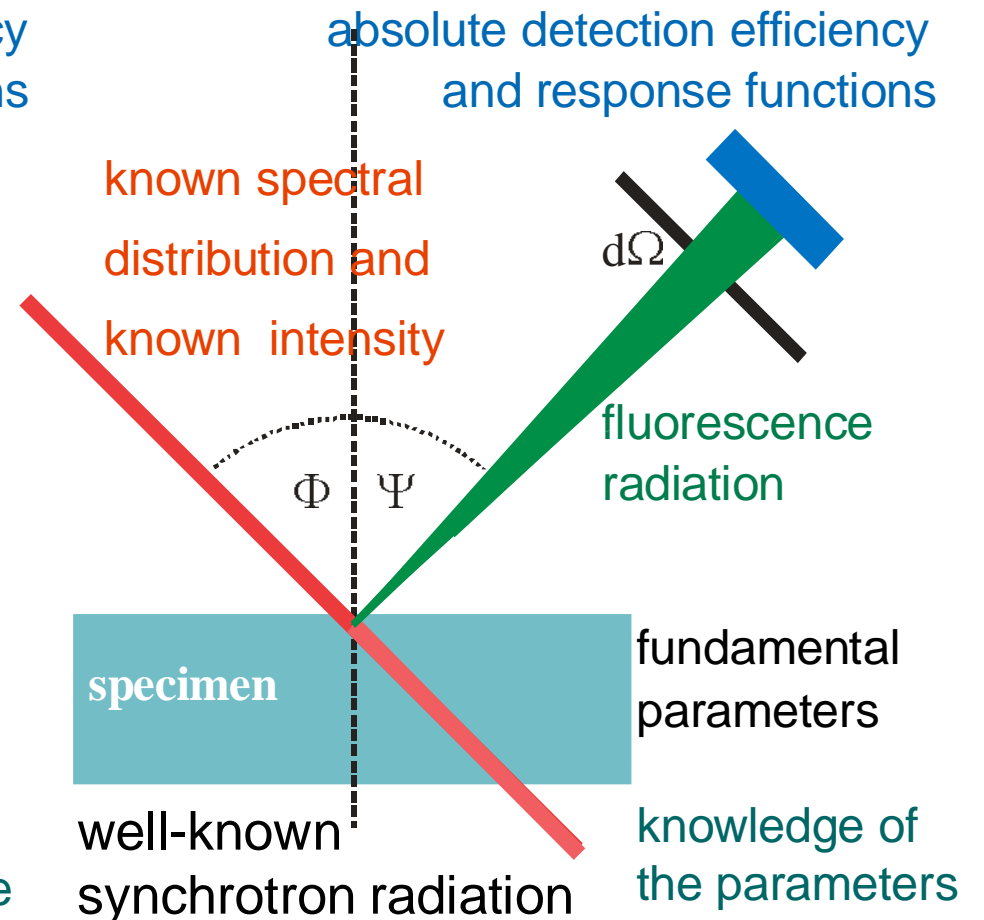
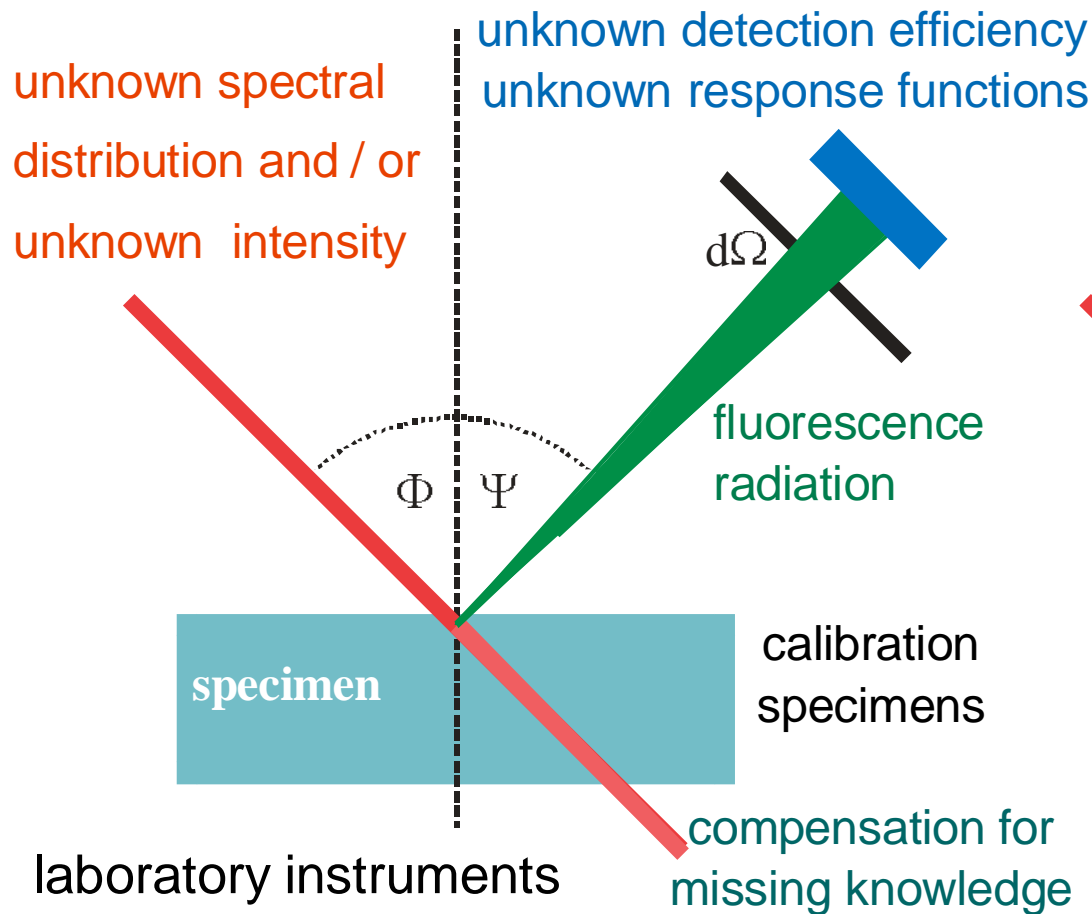
## reference-based versus reference-free approaches



X-ray and IR spectrometry

reference material related technique  
based on well known calibration  
specimens or reference materials

reference-free technique  
based on calibrated instrumen-  
tation and fundamental parameters



# Synchrotron radiation based x-ray spectrometry

XRS excitation channel:

well-known spectral distribution  
and a well-known radiant power

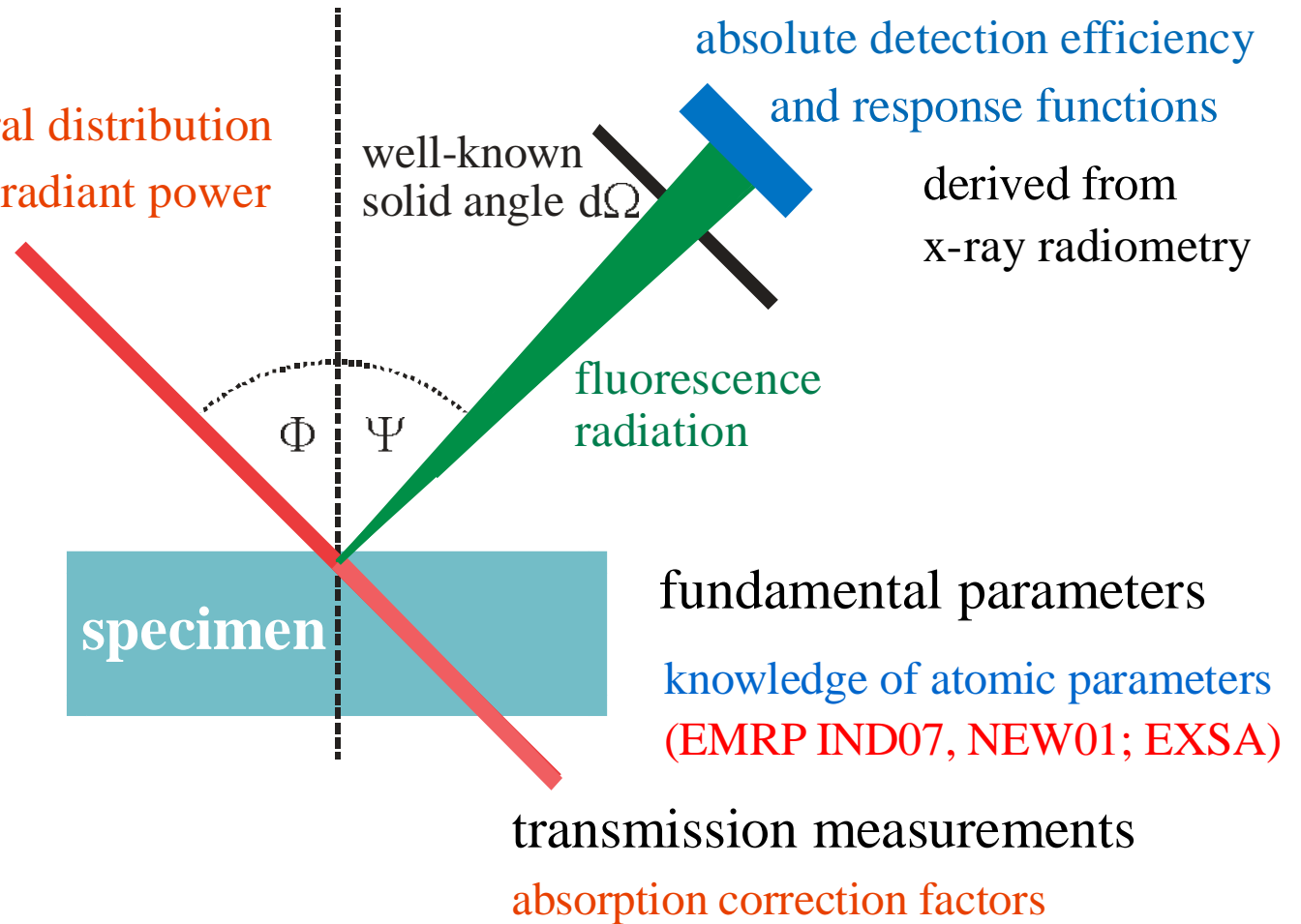
XRS detection channel:

absolute detection efficiency  
and response functions

derived from  
x-ray radiometry

PTB capabilities:

- characterized beamlines
- calibrated photodiodes
- calibrated diaphragms
- calibrated Si(Li) detectors



## Experimental Verification of the Individual Energy Dependencies of the Partial $L$ -Shell Photoionization Cross Sections of Pd and Mo

Philipp Hönicke,<sup>1</sup> Michael Kolbe,<sup>1</sup> Matthias Müller,<sup>1</sup> Michael Mantler,<sup>2\*</sup> Markus Krämer,<sup>3</sup> and Burkhard Beckhoff<sup>1</sup>

<sup>1</sup>*Physikalisch-Technische Bundesanstalt (PTB), Abbestraße 2-12, 10587 Berlin, Germany*

<sup>2</sup>*Rigaku Corporation, 4-14-4, Sendagaya, Shibuya-Ku, Tokyo 151-0051, Japan*

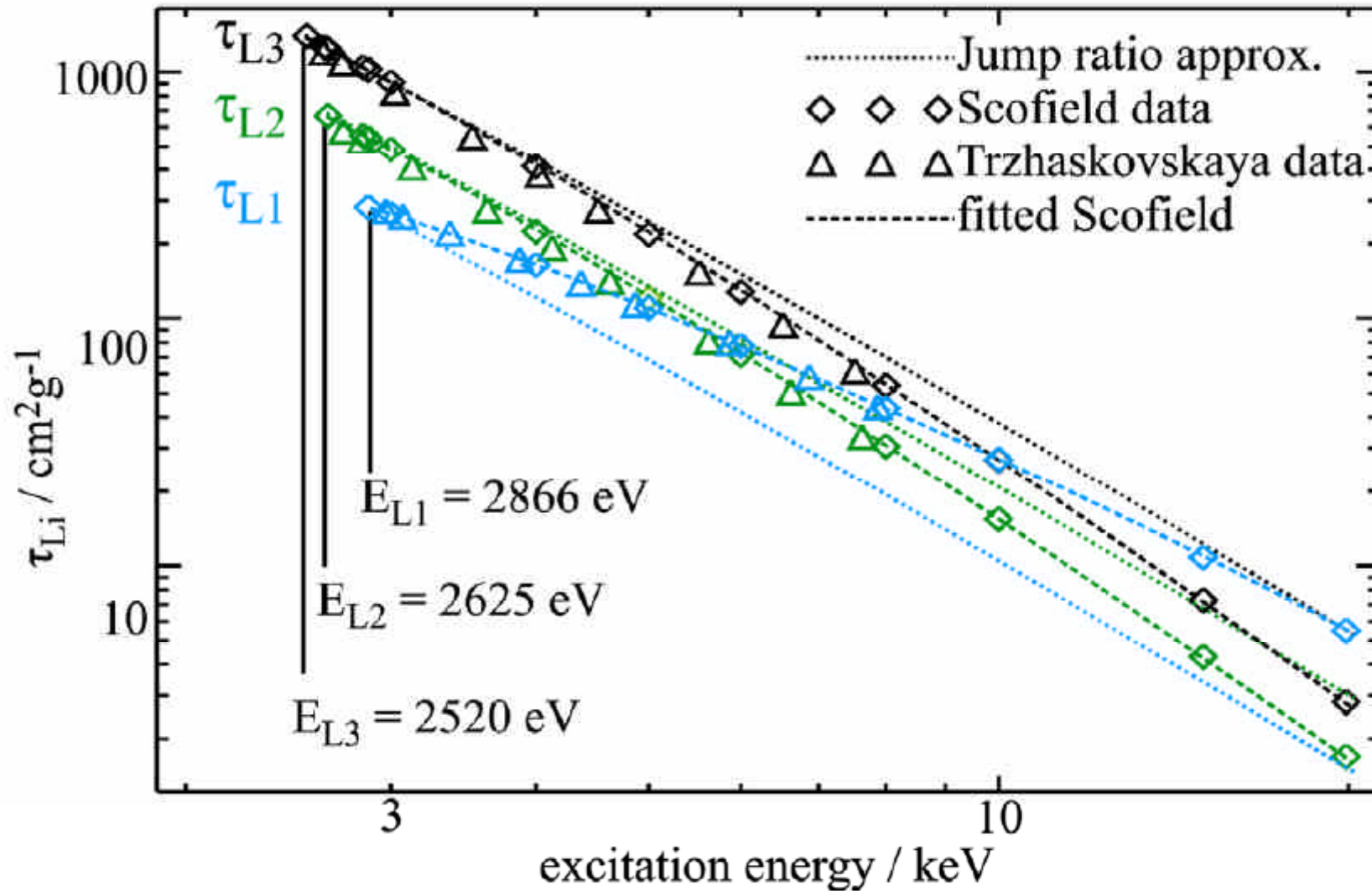
<sup>3</sup>*AXO DRESDEN GmbH, Gasanstaltstraße 8b, 01237 Dresden, Germany*

(Received 17 April 2014; revised manuscript received 9 September 2014; published 13 October 2014)

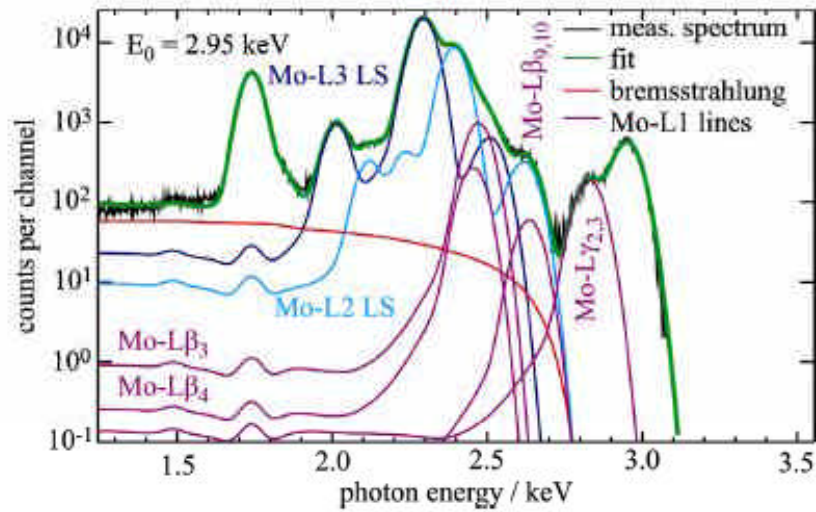
An experimental method for the verification of the individually different energy dependencies of  $L_1$ -,  $L_2$ -, and  $L_3$ - subshell photoionization cross sections is described. The results obtained for Pd and Mo are well in line with theory regarding both energy dependency and absolute values, and confirm the theoretically calculated cross sections by Scofield from the early 1970 s and, partially, more recent data by Trzhaskovskaya, Nefedov, and Yarzhemsky. The data also demonstrate the questionability of quantitative x-ray spectroscopical results based on the widely used fixed jump ratio approximated cross sections with energy independent ratios. The experiments are carried out by employing the radiometrically calibrated instrumentation of the Physikalisch-Technische Bundesanstalt at the electron storage ring BESSY II in Berlin; the obtained fluorescent intensities are thereby calibrated at an absolute level in reference to the International System of Units. Experimentally determined fixed fluorescence line ratios for each subshell are used for a reliable deconvolution of overlapping fluorescence lines. The relevant fundamental parameters of Mo and Pd are also determined experimentally in order to calculate the subshell photoionization cross sections independently of any database.



# Determination of L-shell photoionization cross sections

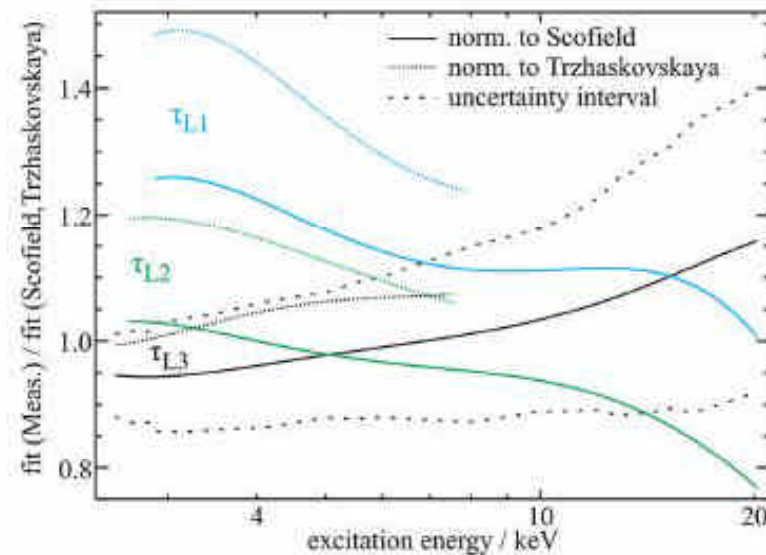
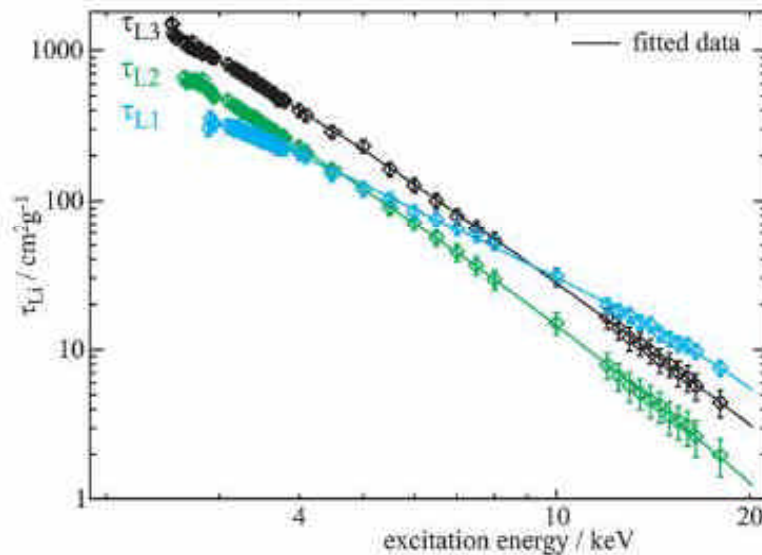


# Determination of L-shell photoionization cross sections



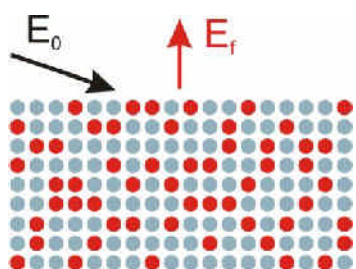
Response function based deconvolution of a Mo layer XRF spectrum for each L-shell.

Experimentally determined PCS for the Mo-L subshells and the comparison to calculated data.



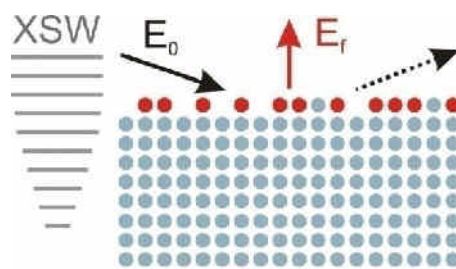
# Tuning the analytical sensitivity and information depth by means of appropriate operational parameters

excitation conditions



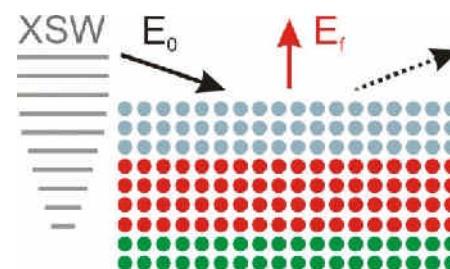
concentration

total-reflection



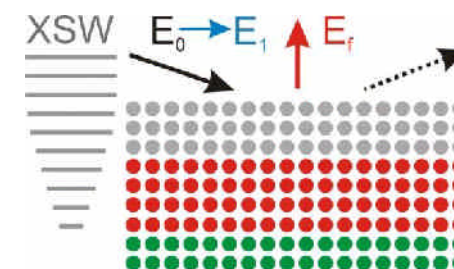
contamination

tunable incident angle



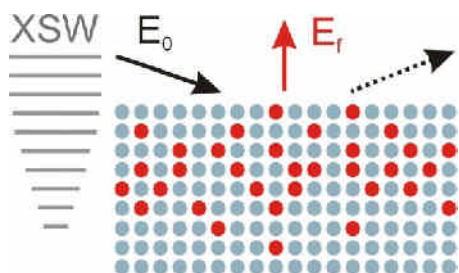
nanolayer

tunable photon energy



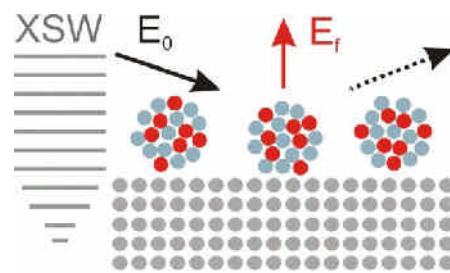
nanolayer speciation

tunable incident angle



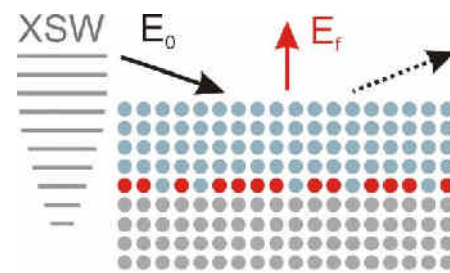
depth profile

total-reflection



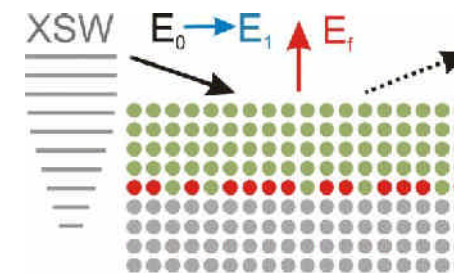
nanoparticles

tunable incident angle



interface

tunable photon energy



interface speciation

$E_0$  = photon energy of excitation radiation

$E_1$  = photon energy above absorption edge

$E_f$  = photon energy of fluorescence radiation

XSW = X-ray Standing Wave field

JAAS 23, 845 (2008)

# How can a method (rows) help another method (columns) to improve or complement the results



X-ray and IR spectrometry

Methods	TXRF	GIXRF	XRF	XRR	XRD	GISAXS
<b>TXRF</b>		surface contamination	information on surface contamination	information on surface contamination	information on surface contamination	nanoparticle composition
<b>GIXRF</b>	absolute angle calibration		validation measurands	near surface depth profiles	near surface depth profiles	nanoparticle composition
<b>XRF</b>	validation measurands	validation measurands		information on material composition	information on material composition	nanoparticle composition
<b>XRR</b>	layer thickness and roughness for modelling	layer thickness and roughness for modelling	contaminations/spectral diffraction artefact		layer thickness, roughness, density	substrate surface layer
<b>XRD</b>	information on material morphology, artefacts	information on material morphology, artefacts	information on material morphology, artefacts	information on material morphology		information on material morphology
<b>GISAXS</b>	particle size distribution	particle size distribution	_____	particle size distribution	particle size distribution	

# Typical characteristics and properties of x-ray analytical and metrology techniques



X-ray and IR spectrometry

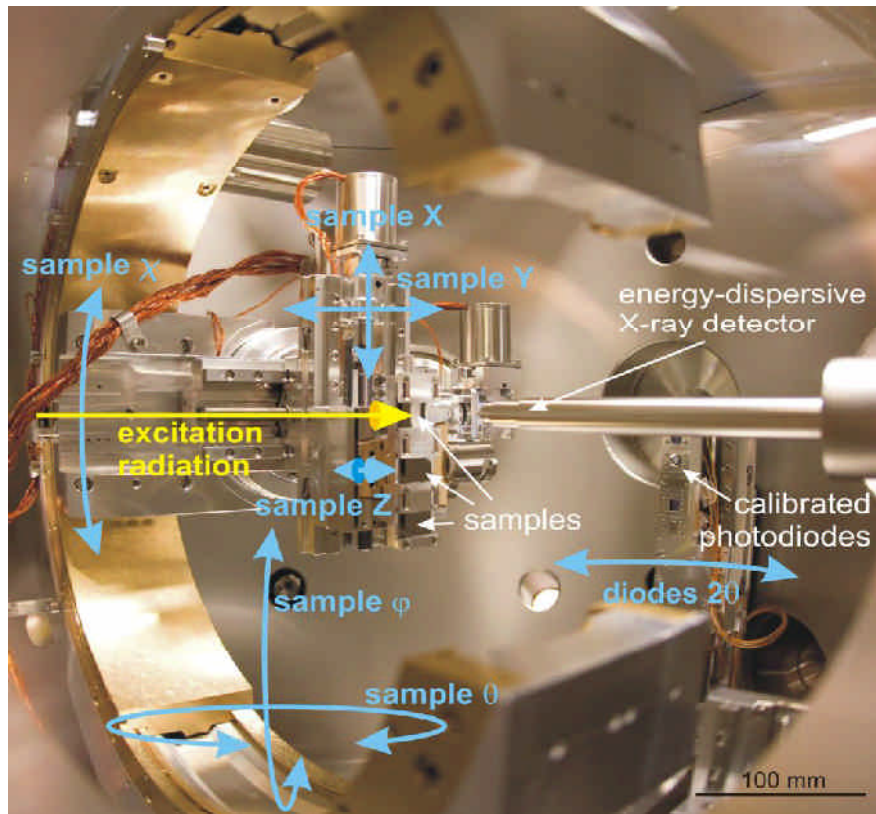
	TXRF	GIXRF	XRF	XRR	XRD	GISAXS
Applications	surfaces	nanolayers, elemental depth profiles, implantation profiles	bulk materials	nano layers	thin layers	nano structured surfaces, thin films
Properties to be measured	mass density in the range of the elements B to U	mass density, concentration, depth profile in the range of the elements B to U	mass density in the range of the elements B to U	layer thickness, roughness, density	layer thickness, orientation	particle size
Detection limit	app. $10^{10}$ atoms/ cm <sup>2</sup>	app. $10^{12}$ atoms/ cm <sup>2</sup>	app. $10^{13}$ atoms/ cm <sup>2</sup>	2 nm – 5 nm	3 wgt.%, 2 nm	2 nm
Range	$10^{10}$ atoms/ cm <sup>2</sup> - $10^{15}$ atoms/ cm <sup>2</sup>	$10^{12}$ atoms/ cm <sup>2</sup> - $10^{17}$ atoms/ cm <sup>2</sup>	ppb – %	5- 500 nm	0.1 nm – 10 nm	2 nm – 1µm
Accuracy (and reproducibility ) (*reference free)	0.15* / 0,05 (0.02)	0.2*/0.05 (0.03)	0.2*/0.05 (0.03)	0.02 (0.01)	0.05 (0.02)	0,15 (0.02)
Spatial resolution	1 mm <sup>2</sup> -1 cm <sup>2</sup>	0.5 mm <sup>2</sup> -0.5 cm <sup>2</sup>	to 1 mm <sup>2</sup>	to 1 mm <sup>2</sup>	0.5 mm <sup>2</sup> -0.5 cm <sup>2</sup>	0.5 mm <sup>2</sup> -0.5 cm <sup>2</sup>
Measurement speed	50 s – 1000 s/ pt	2000 s – 5 h	100 s – 1000 s	1000 s – 5 h	1000 s – 5 h	10 min/frame

# Novel XRS instrumentation for advanced materials characterizations with synchrotron radiation



X-ray and IR spectrometry

## PTB XRS instrumentation at BESSY

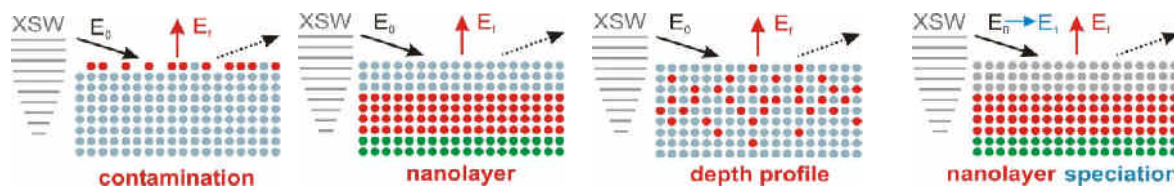


## 9-axis manipulator and chamber ensuring

- the entire TXRF, GIXRF and XRF regime
- polarization-dependent speciation by XAFS
- combined GIXRF and XRR investigations
- movable aperture system for reference-free XRF and atomic FP determinations

## Transfer of modified instrumentation to

- TU Berlin for a **laboratory plasma source**
- LNE/CEA-LNHB for **SOLEIL storage ring**
- IAEA (UN) for **ELETTRA storage ring**



Janin Lubeck et al.,

Rev. Sci. Instrum. **84**, 045106 (2013)

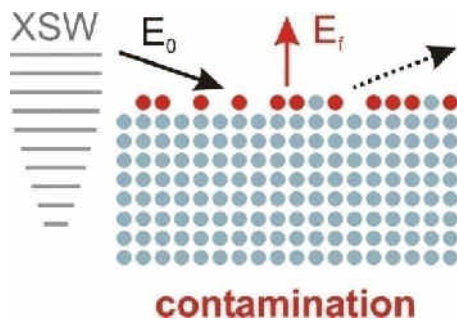
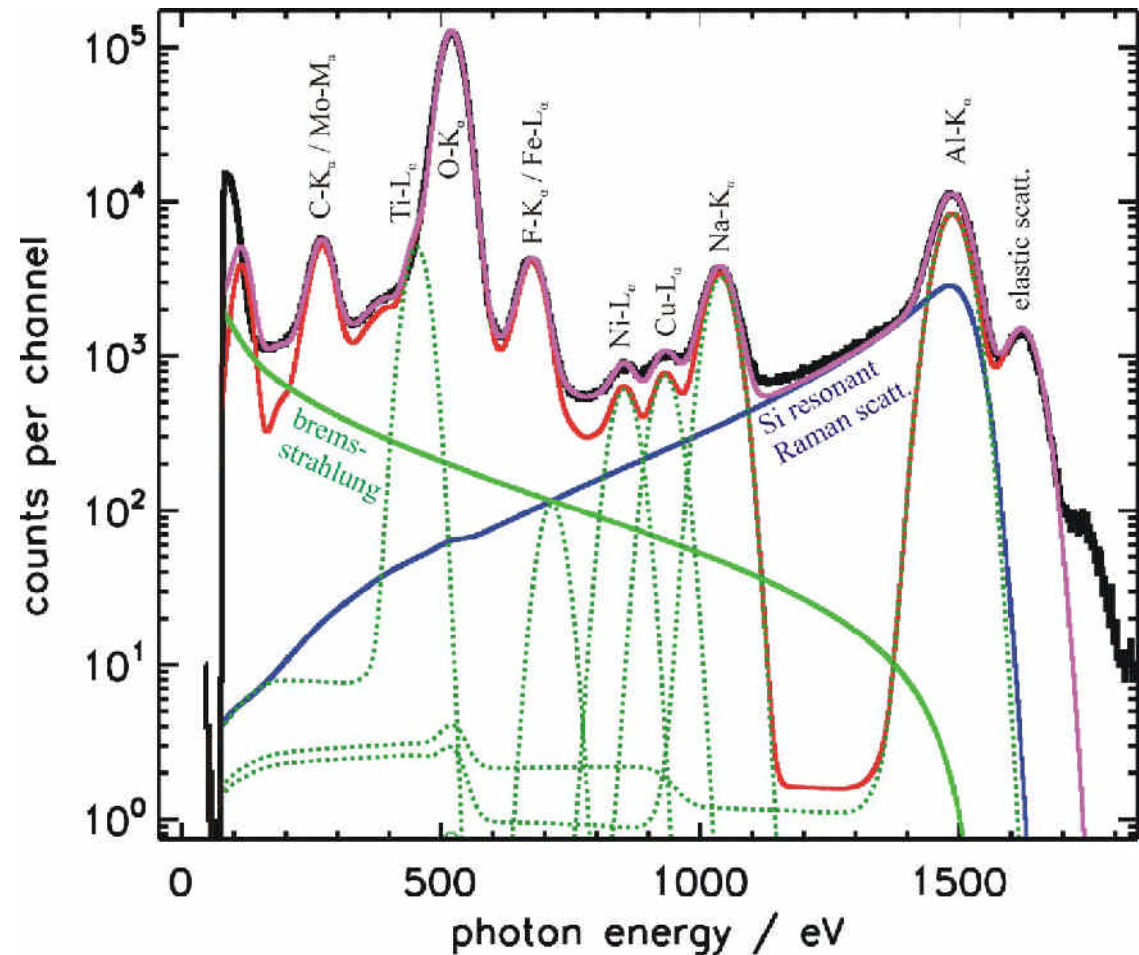
# Quantitation in SR-TXRF routine analysis on Si wafers

## TXRF spectra deconvolution

including Si(Li) detector response functions, RRS, and bremsstrahlung contributions.

reference-free TXRF quantitation: known incident flux, detector efficiency and solid angle.

spin-coated wafer with  $10^{12}$  cm<sup>-2</sup> of various transition metals



## Reference-free quantitation in SR-TXRF analysis

mass deposition  $m_i / F_I$  of the element  $i$  with unit area  $F_I$

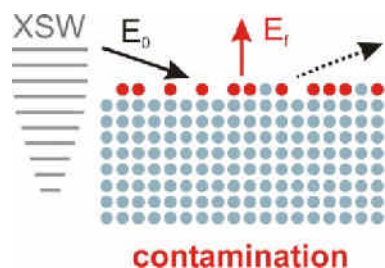
$$\frac{m_i}{F_I} = \frac{-1}{\mu_{tot,i}} \ln \left\{ 1 - \frac{P_i}{P_{0,Wsurf} \tau_{i,E_0} Q \frac{\Omega_{det}}{4\pi} \frac{1}{\sin \psi_{in}} \frac{1}{\mu_{tot,i}}} \right\}$$

$E_0$  photon energy of the incident (excitation) radiation

$P_0 = S_0 / \sigma_{diode,E_0}$  radiant power of the incident radiation

$S_0$  signal of the photodiode measuring the incident radiation

$\sigma_{diode,E_0}$  spectral responsivity of the photodiode





# Reference-free quantitation in SR-TXRF analysis

mass deposition  $m_i / F_I$  of the element  $i$  with unit area  $F_I$

$$\frac{m_i}{F_I} = \frac{-1}{\mu_{tot,i}} \ln \left\{ 1 - \frac{P_i}{P_{0,Wsurf} \tau_{i,E_0} Q \frac{\Omega_{det}}{4\pi} \frac{1}{\sin \psi_{in}} \frac{1}{\mu_{tot,i}}} \right\}$$

$I_{Wsurf}$

relative intensity of the X-ray standing wave field<sup>1</sup> at the wafer surface

$$P_{0,Wsurf} = P_0 I_{Wsurf}$$

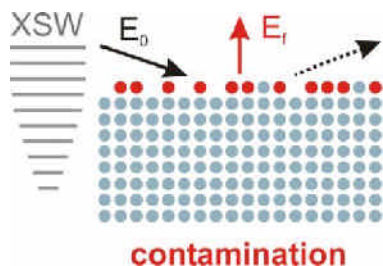
<sup>1</sup> software package IMD: D. Windt, Computers in Physics **12**, 360-370 (1998)

$\psi_{in}$

angle of incidence with respect to the wafer surface

$E_i$

photon energy of the fluorescence line  $l$  of the element  $i$



## Reference-free quantitation in SR-TXRF analysis

mass deposition  $m_i / F_I$  of the element  $i$  with unit area  $F_I$

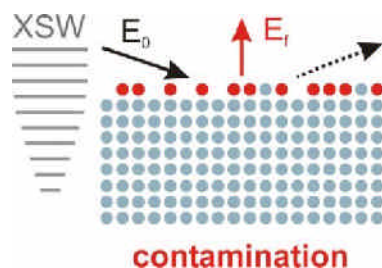
$$\frac{m_i}{F_I} = \frac{-1}{\mu_{tot,i}} \ln \left\{ 1 - \frac{P_i}{P_{0,Wsurf} \tau_{i,E_0} Q \frac{\Omega_{det}}{4\pi} \frac{1}{\sin \psi_{in}} \frac{1}{\mu_{tot,i}}} \right\}$$

$R_i$  detected count rate of the fluorescence line  $l$  of the element  $i$

$\varepsilon_{det,E_i}$  detection efficiency of the Si(Li) detector at the photon energy  $E_i$

$$P_i = R_i / \varepsilon_{det,i}$$

$\Omega_{det}$  effective solid angle of detection



## Reference-free quantitation in SR-TXRF analysis

mass deposition  $m_i / F_I$  of the element  $i$  with unit area  $F_I$

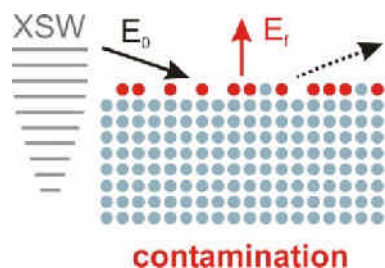
$$\frac{m_i}{F_I} = \frac{-1}{\mu_{tot,i}} \ln \left\{ 1 - \frac{P_i}{P_{0,Wsurf} \tau_{i,E_0} Q \frac{\Omega_{det}}{4\pi} \frac{1}{\sin \psi_{in}} \frac{1}{\mu_{tot,i}}} \right\}$$

$\psi_{out}$  angle of observation which equals  $90^\circ$  in a typical TXRF geometry

$\tau_{i,E_0}$  photo electric cross section of the element  $i$  at the photon energy

$\mu_{i,E}$  absorption cross section of the element  $i$  at the photon energy  $E$

$$\mu_{tot,i} = \mu_{i,E_0} / \sin \psi_{in} + \mu_{i,E_i} / \sin \psi_{out}$$



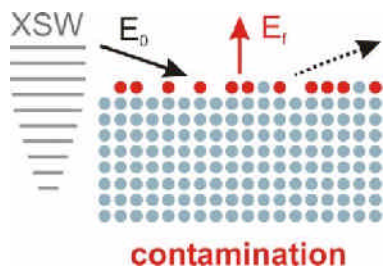
# Reference-free quantitation in SR-TXRF analysis

mass deposition  $m_i / F_I$  of the element  $i$  with unit area  $F_I$

$$\frac{m_i}{F_I} = \frac{-1}{\mu_{tot,i}} \ln \left\{ 1 - \frac{P_i}{P_{0,Wsurf} \tau_{i,E_0} Q \frac{\Omega_{det}}{4\pi} \frac{1}{\sin \psi_{in}} \frac{1}{\mu_{tot,i}}} \right\}$$

- $\omega_{Xi}$  fluorescence yield of the absorption edge  $Xi$  (of the element  $i$ )
- $g_{l, Xi}$  transition probability of the fluorescence line  $l$  belonging to  $Xi$
- $j_{Xi}$  jump ratio at the absorption edge  $Xi$

$$Q = \omega_{Xi} g_{l, Xi} (j_{Xi} - 1) / j_{Xi}$$



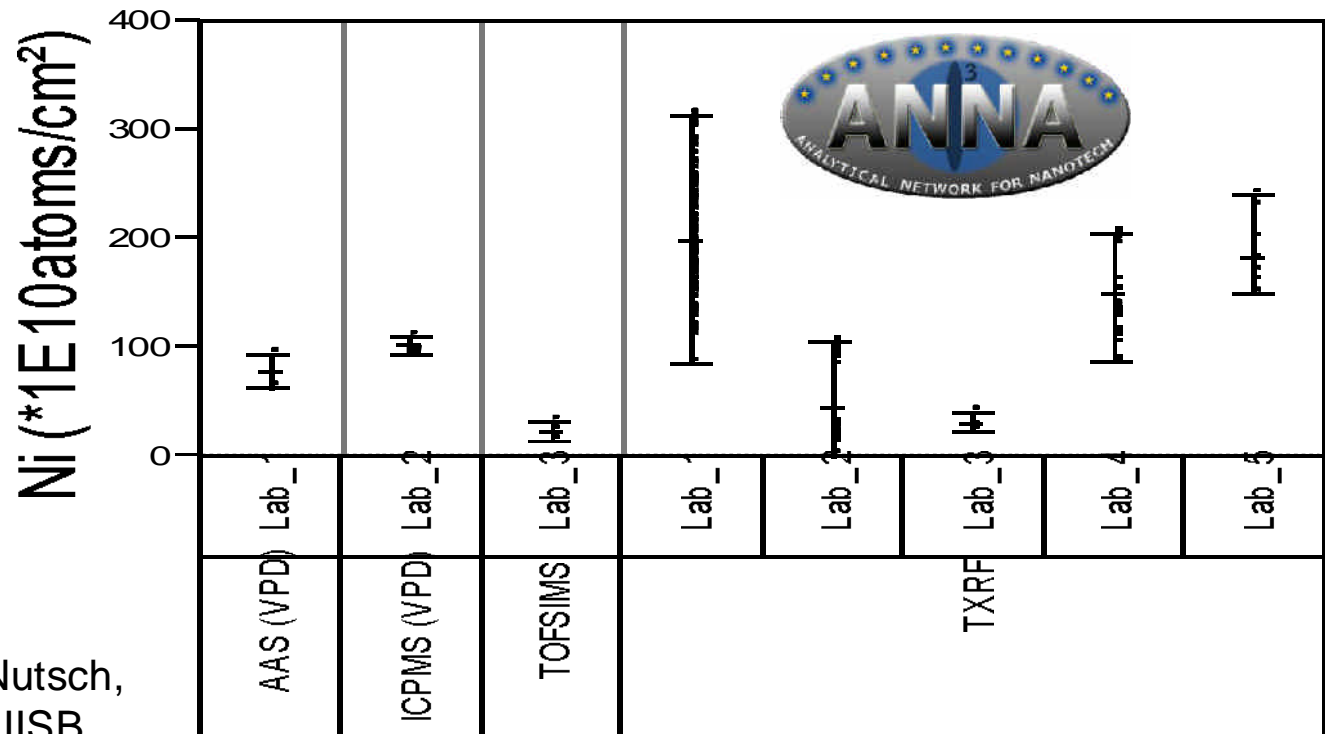
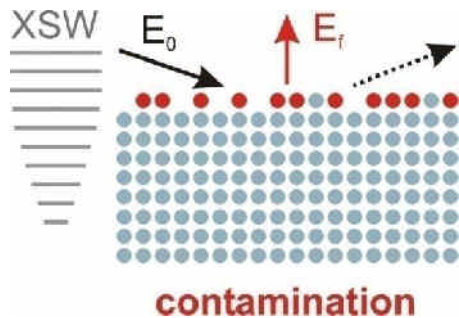
Analysis of contamination on novel materials (Ge, SOI, InGaAs, ...) or of nanolayered systems (buried interfaces – photovoltaics )  
 → calculation of the x-ray standing wave field

# reference based TXRF - Ni surface contamination

Total-reflection X-ray Fluorescence (TXRF) analysis:

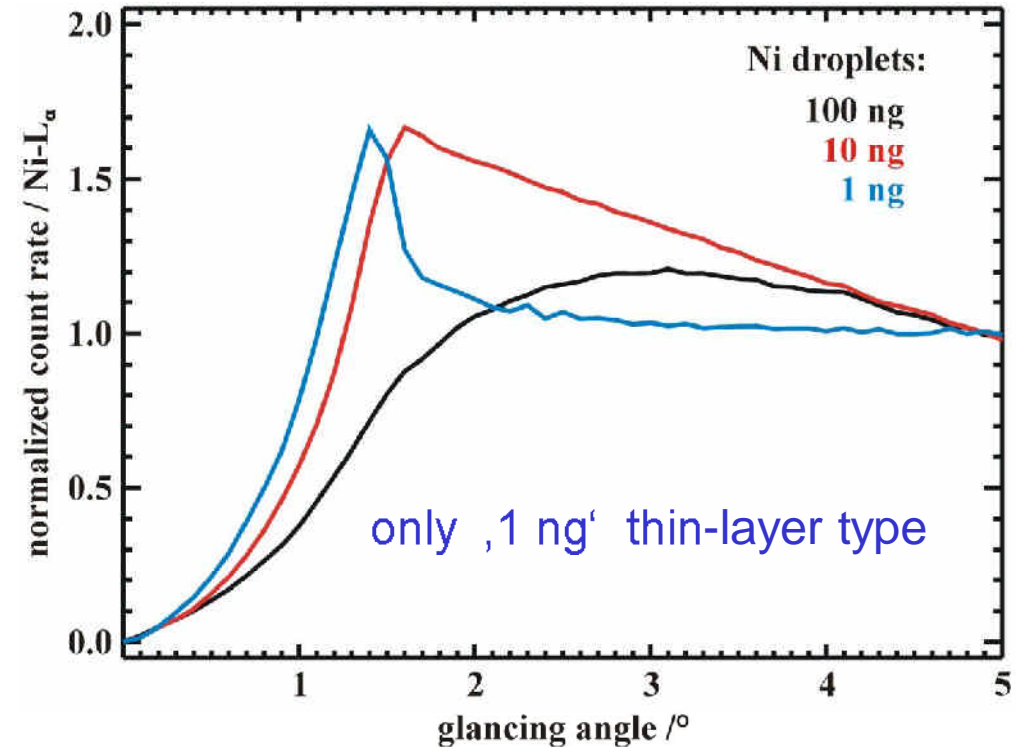
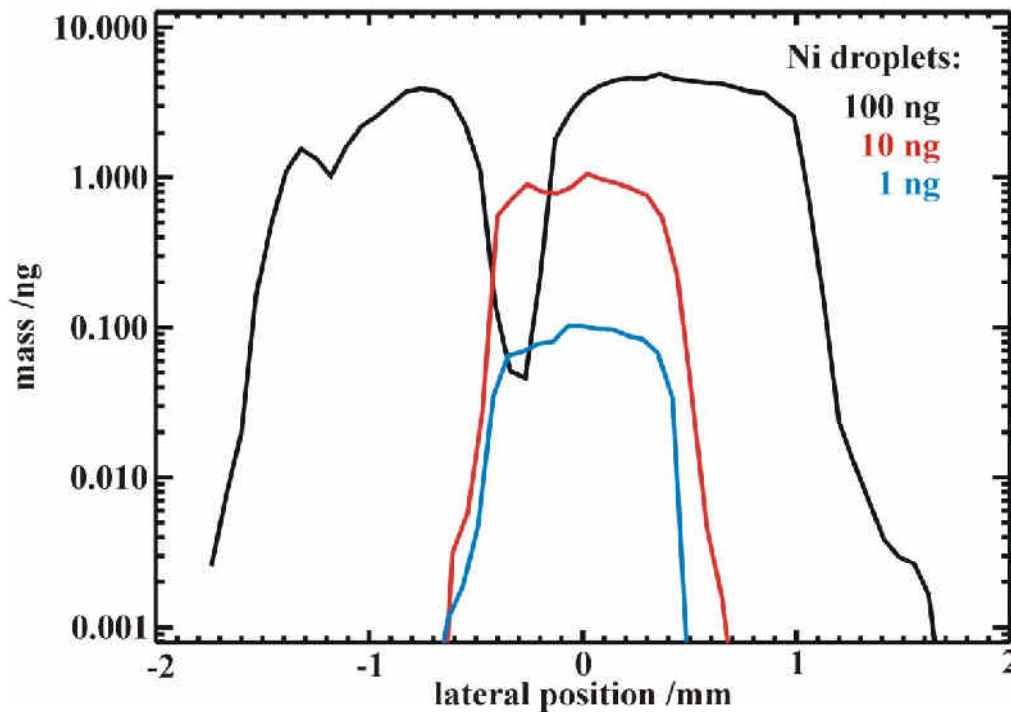
- non-consistent results from round robin tests (differences up to a factor of ten)
- reason: problems with employed calibration samples (droplet depositions)

spin coated contamination:  
 metals  $1 \times 10^{12}$  atoms/cm<sup>2</sup>  
 and light elements (Na, Al)  
 $1 \times 10^{13}$  atoms/cm<sup>2</sup>



A. Nutsch,  
FhG IISB

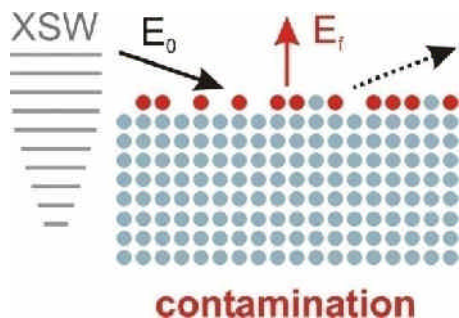
# Assessment of TXRF calibration samples for Ni surface contamination



Reason for deviations in contamination results: inhomogeneities

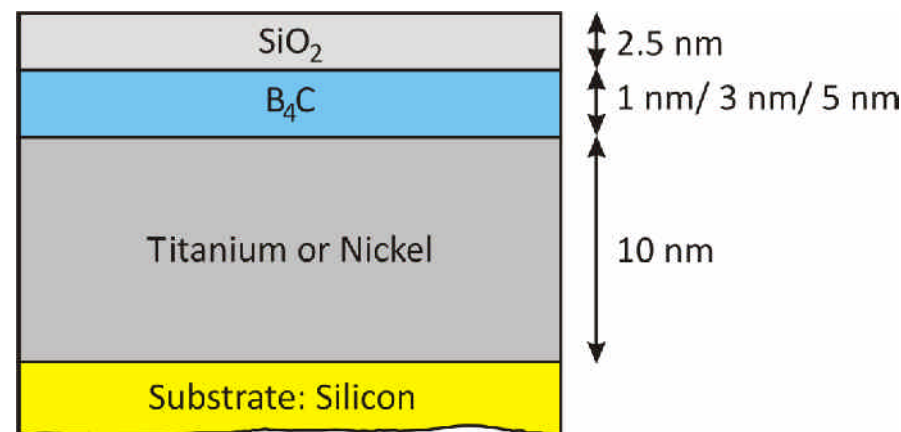
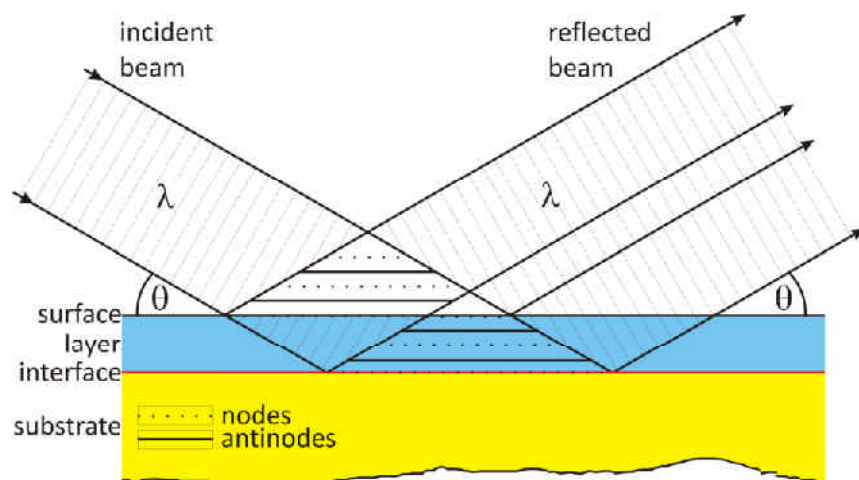
and absorption saturation of TXRF calibration droplets

→ “slicing” and “angular scanning” of calibration droplets by reference-free TXRF as validation technique



# Reference-free XRF and grazing-incidence XRF of buried nanolayers - layer composition and thickness

## X-ray standing wave field (XSW)

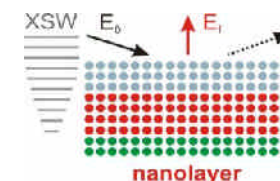


design of samples: total-reflection of the incident beam at silicon or at the metal

→ occurrence of the XSW in boron carbide layer

objective: determination of the boron carbide layer composition and thickness

→ comparison of XRF and GIXRF quantification

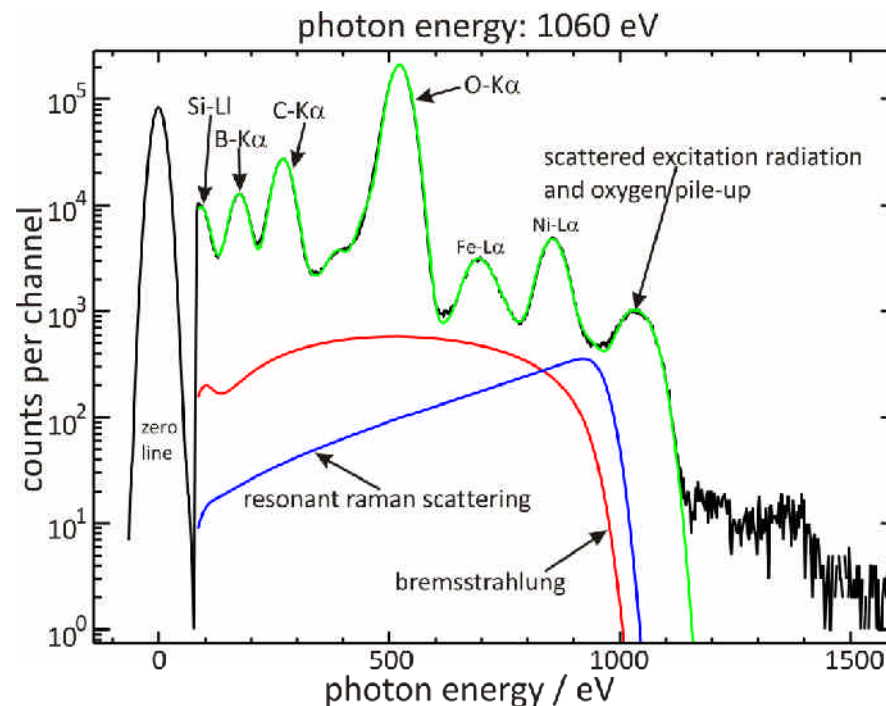
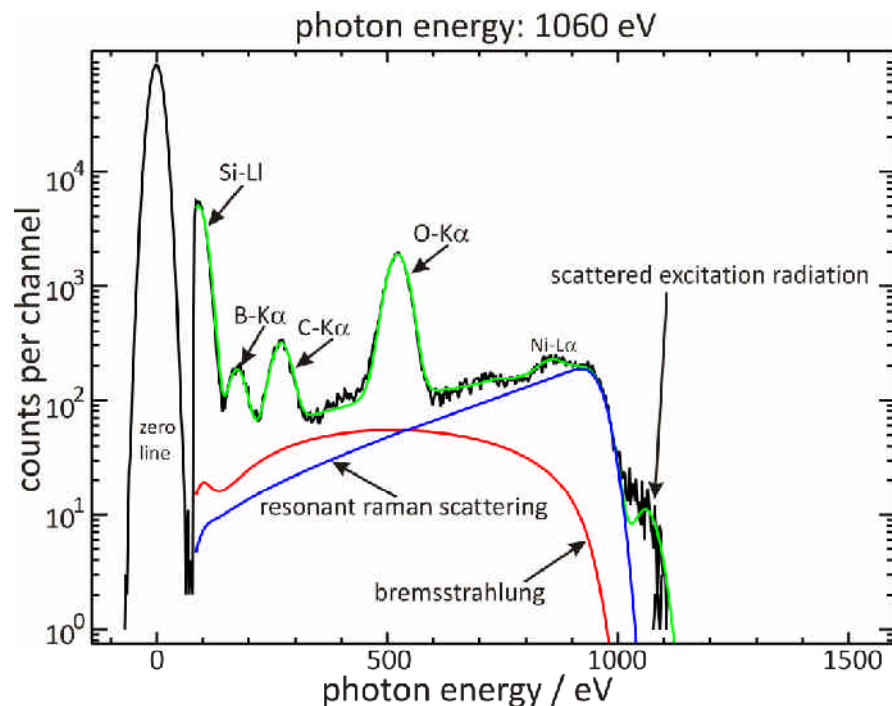


# Reference-free XRF and grazing-incidence XRF of buried nanolayers - layer composition and thickness



X-ray and IR spectrometry

sample: nominal 2.5 nm SiO<sub>2</sub> / 5 nm B-C / Si-substrate

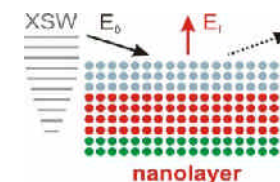


signal to background: XRF 3:1

GIXRF 130:1

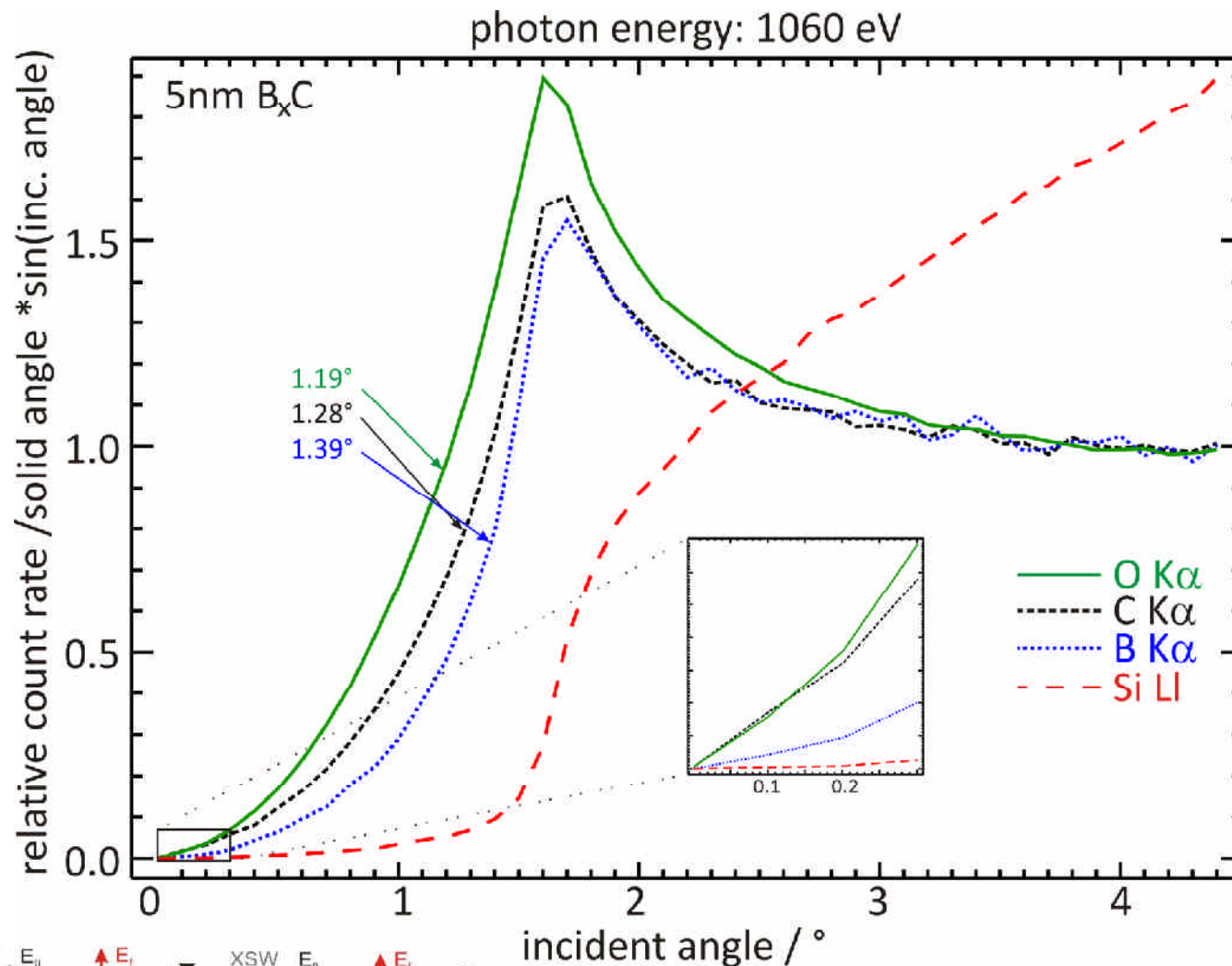
quantification reliability better for XRF

Anal. Chem. **83**, 8623 (2011)





# Reference-free XRF and grazing-incidence XRF of buried nanolayers - layer composition and thickness



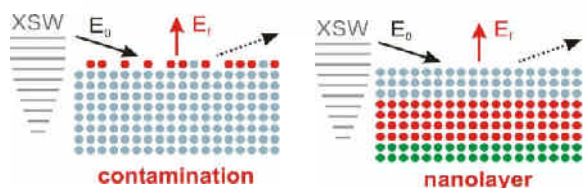
depth-dependent modification of the excitation radiation due to XSW



reveal information about the sequence of the layers

1. oxygen
2. carbon
3. boron
4. silicon (substrate)

carbon contamination at surface recorded



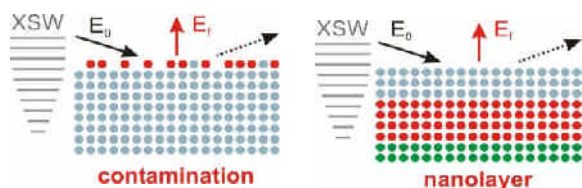
# Reference-free XRF and grazing-incidence XRF of buried nanolayers - layer composition and thickness

B-layer thickness	without Ti/Ni-layer /nm	with 10nm Ti-layer /nm	with 10nm Ni-layer /nm
nominal 0.8 nm B	0.9 ± 0.3 0.9 ± 0.2	0.7 ± 0.2 0.8 ± 0.2	0.6 ± 0.4 1.0 ± 0.3
nominal 2.5 nm B	2.5 ± 0.8 2.6 ± 0.7	2.4 ± 0.7 2.5 ± 0.7	2.0 ± 1.0 2.7 ± 0.7
nominal 4.2 nm B	4.0 ± 1.2 4.2 ± 1.1	3.9 ± 1.2 4.0 ± 1.0	3.5 ± 1.8 4.3 ± 1.1

GIXRF  
XRF

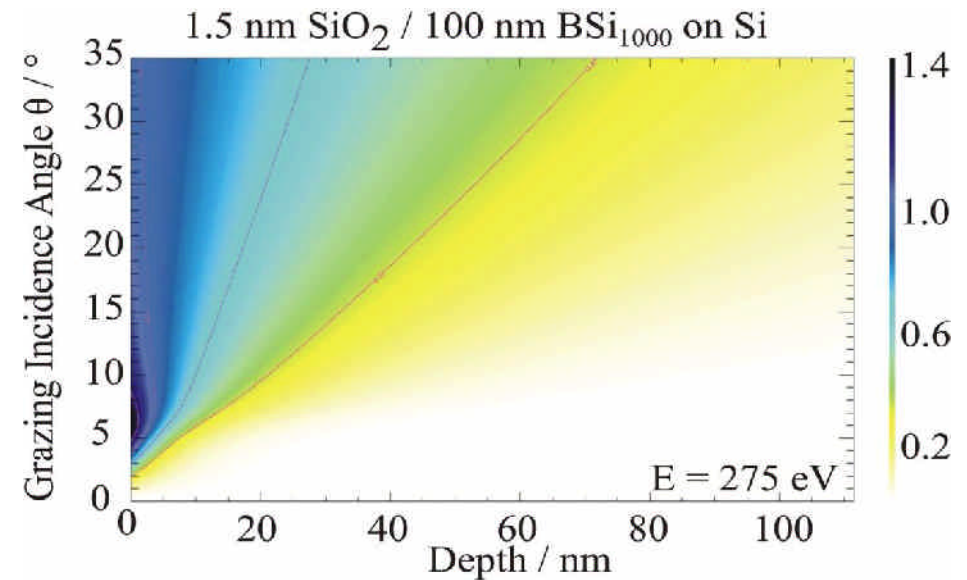
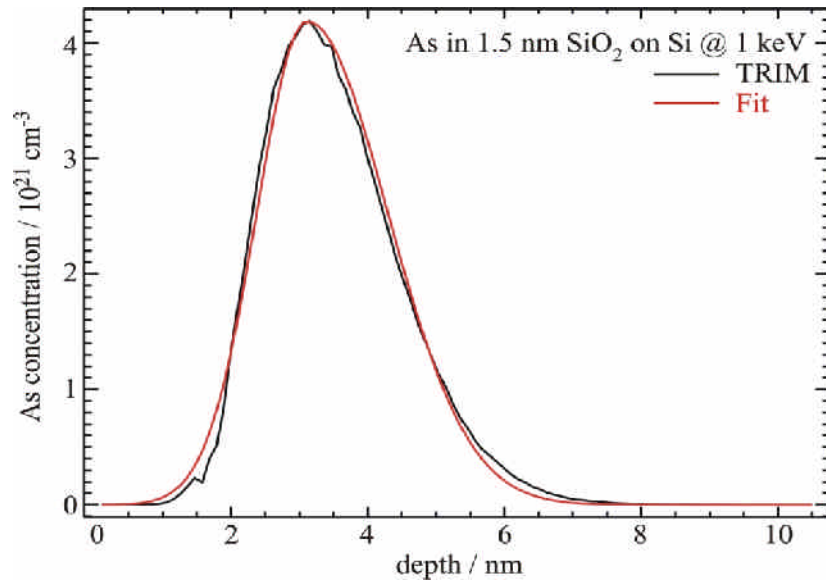
determined thicknesses at 510 eV excitation in line with nominal values deviations

→ relevant influence of XSW and surface carbon contamination



Anal. Chem. **83**, 8623 (2011)

# GIXRF analysis of B and As implantation profiles

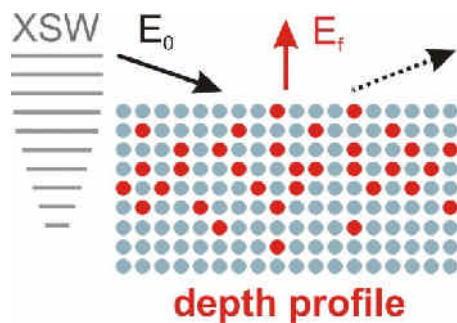


fundamental and instrumental parameters

depth distribution of the implant

X-ray Standing Wave field distribution

absorption term



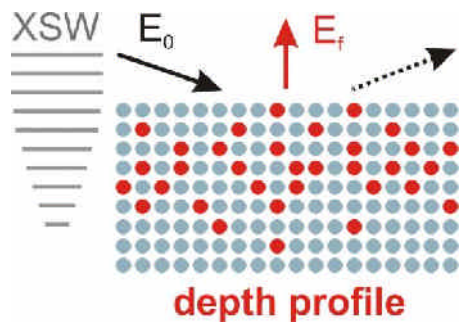
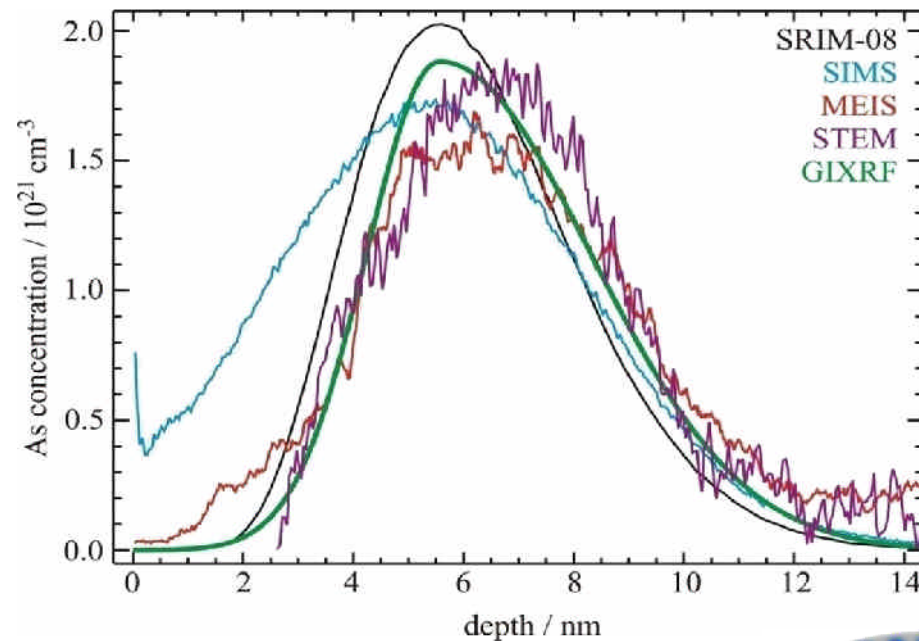
$$F_{Imp}(\theta) = G \int_0^{t_{max}} P_{Imp}(t) \cdot I_{XSW}(t, \theta, E_0) \cdot \left( e^{-\frac{t \rho \mu_{tot}(t)}{\sin \theta_{det}}} \right) dt$$

P. Hönicke

Anal. Bioanal. Chem. **396**, 2825 (2010)

# GIXRF analysis of B and As implantation profiles

Comparison of GIXRF results on arsenic samples to SIMS, MEIS and STEM

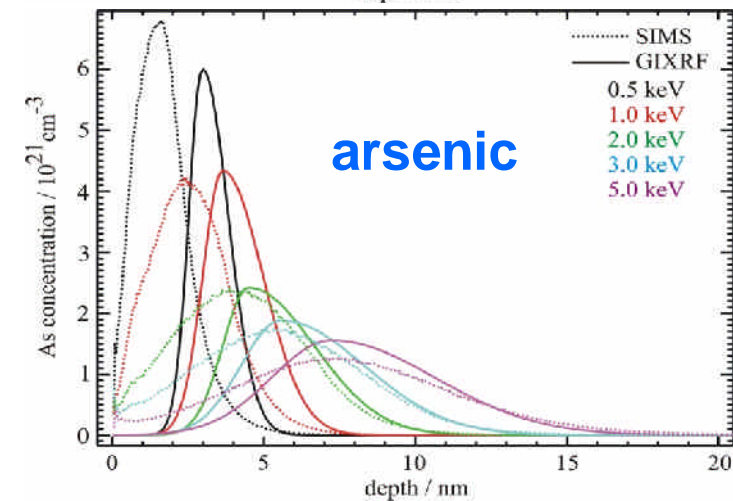
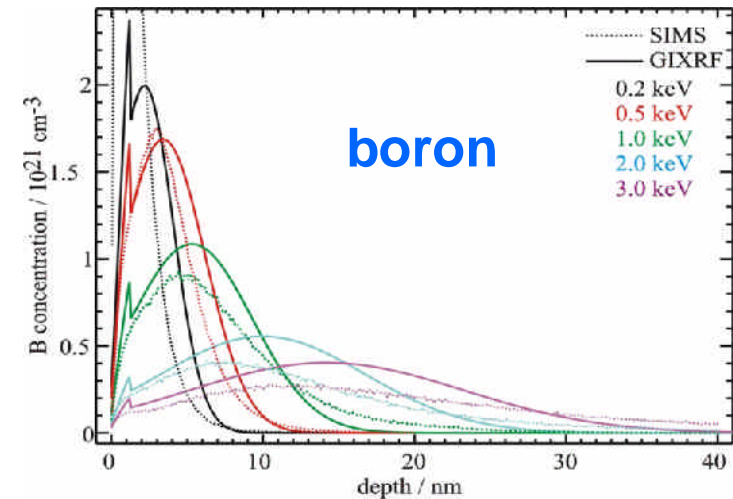


D. Giubertoni (FBK)

J. van den Berg (Univ. Salford)

P. Hönicke

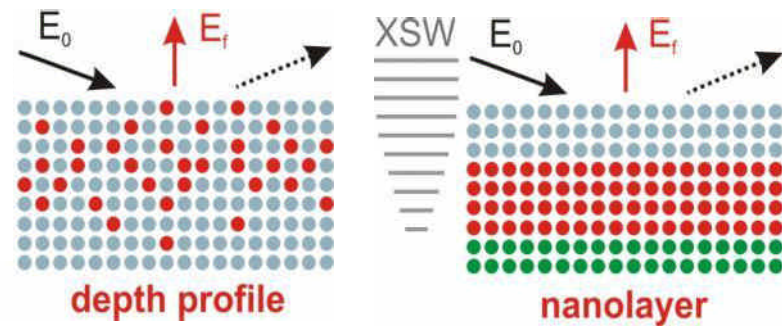
Comparison of GIXRF results to SIMS



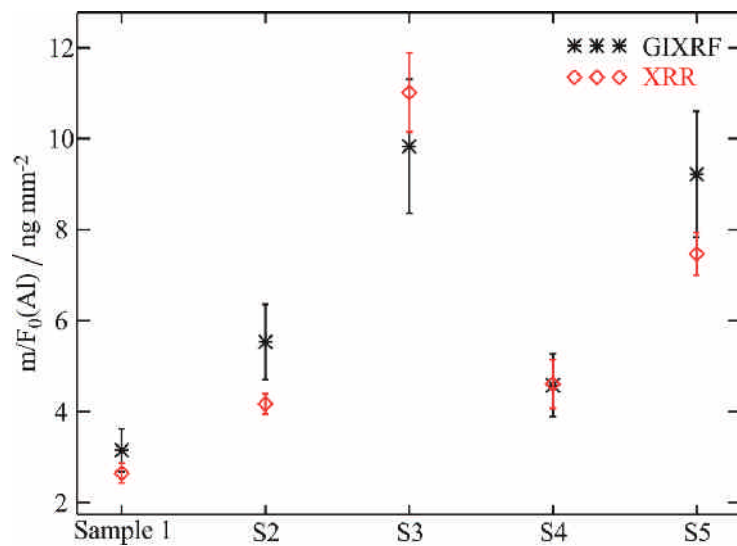
[Anal. Bioanal. Chem. 396, 2825 \(2010\)](#)

# XRR enhanced GIXRF depth profiling

- GIXRF can be used to depth profile gradient (e.g. ion implants) or nanolayered samples
- iterative calculation of the XSW using X-ray reflectivity data for reliable modeling

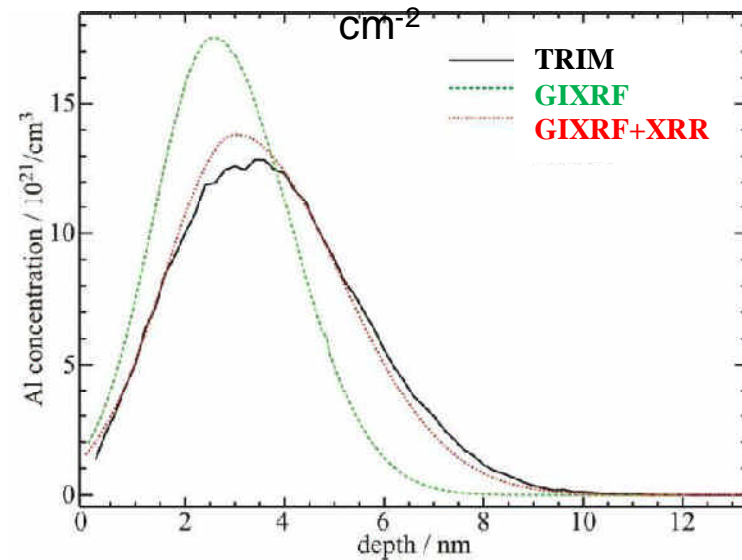


Al<sub>2</sub>O<sub>3</sub> / HfO<sub>2</sub> nanolaminates



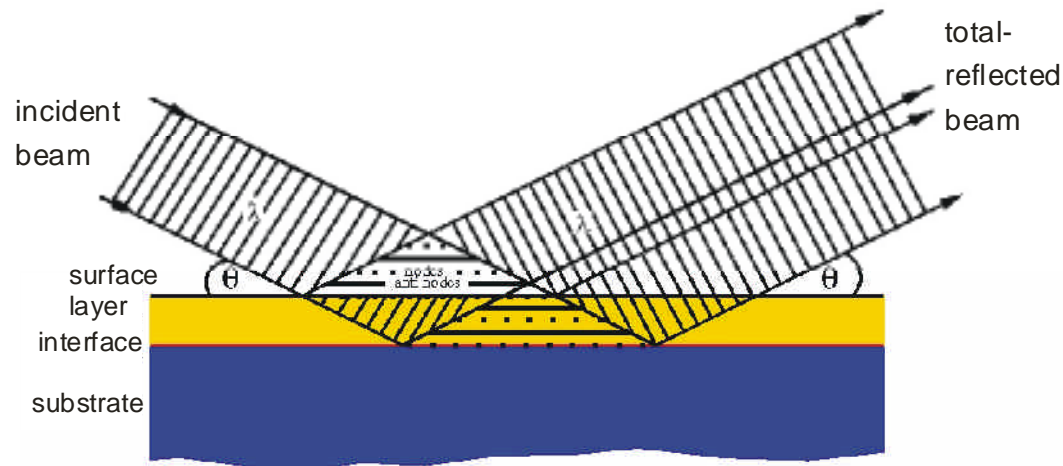
XRR not matching reference-free GIXRF

1 keV Al implant into Si, dose: 10<sup>16</sup>



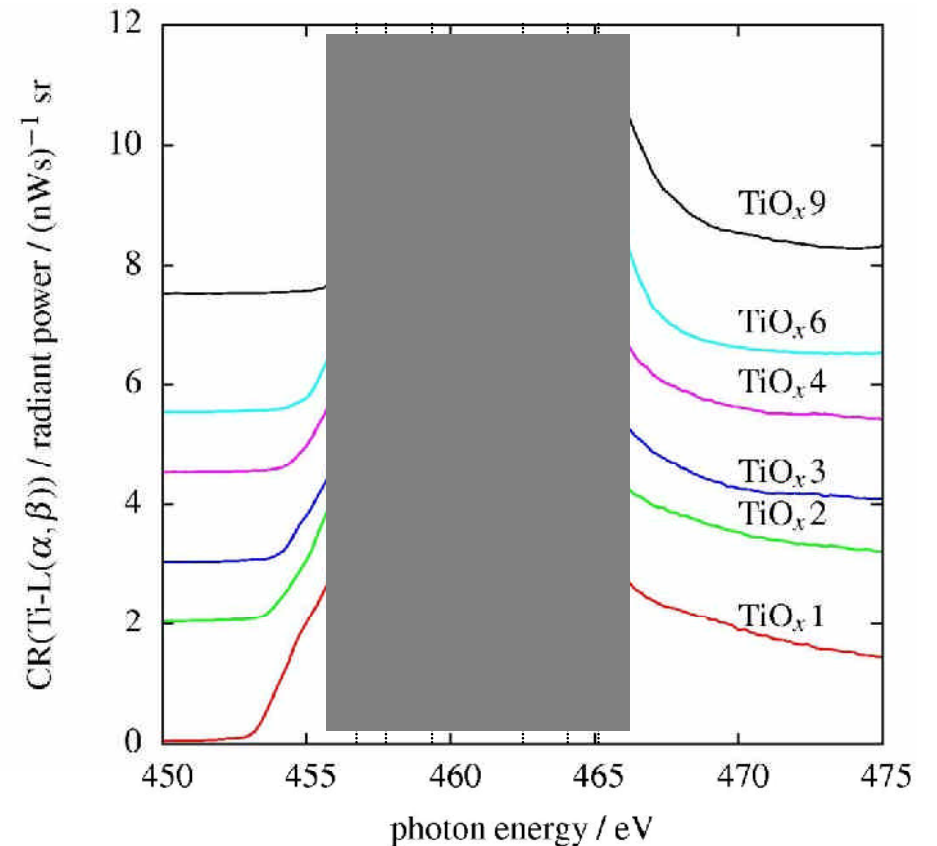
Combining XRR and GIXRF improves result

# Speciation of buried nanolayers by GIXRF-NEXAFS

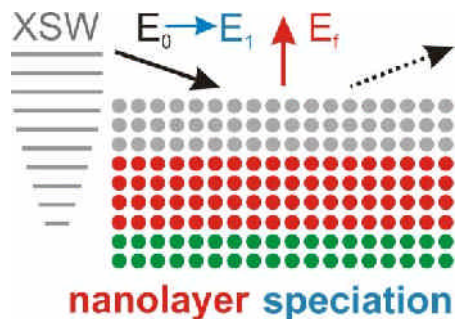


- composition and speciation of buried nanolayers
- higher information depth ( $\gg 5\text{nm}$ ) than XPS
- parallel variation of incident angle and photon energy

## GIXRF-NEXAFS at the Ti-L<sub>iii,ii</sub> edges



**speciation of buried Ti oxide nanolayers**  
(the degree of oxidation scales with indices)



B. Pollakowski

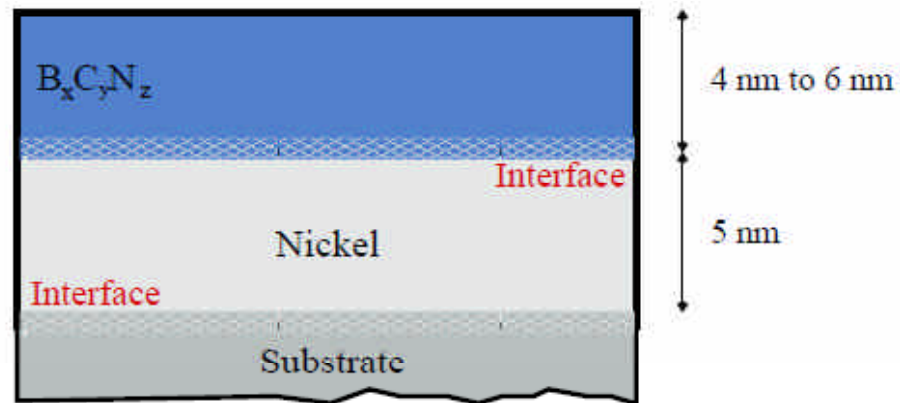
Phys. Rev. B **77**, 235408 (2008)

Anal. Chem. **85**, 193 (2013)

# Speciation of buried interfaces by GIXRF-NEXAFS

## Further developing GIXRF-NEXAFS for interfacial speciation

- Nickel layer deposited with PVD technique,  $B_xC_yN_z$  with CVD technique
- Variation of the temperature in the CVD process



No.	Temperature $B_xC_yN_z$ $T / ^\circ C$
1	200
2	300
3	500



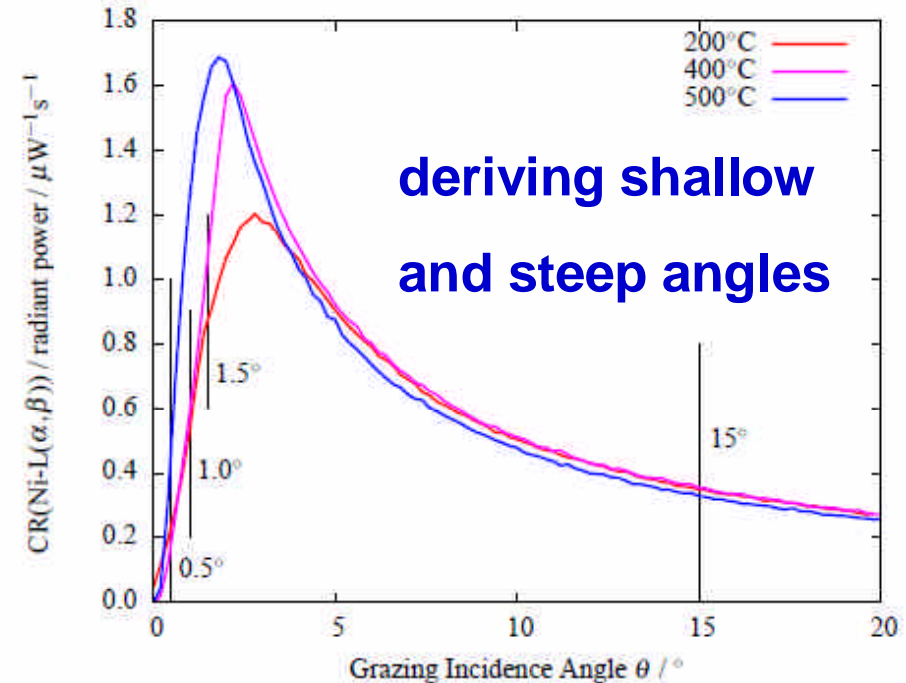
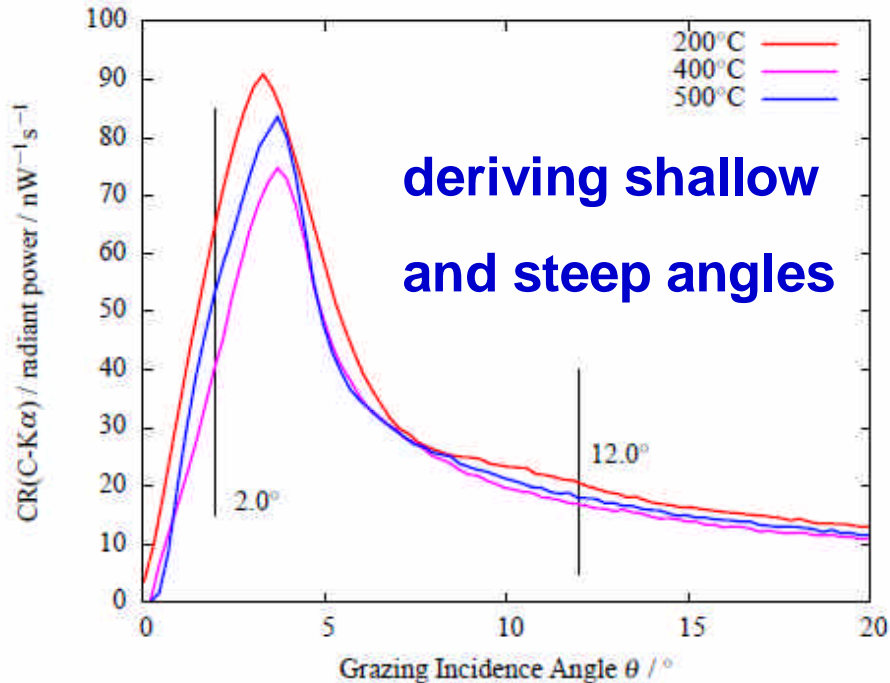
B. Pollakowski

Anal. Chem. **85**, 193 (2013)

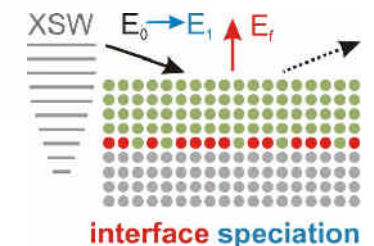
# Speciation of buried interfaces by GIXRF-NEXAFS

photon energy: 510 eV

photon energy: 1060 eV

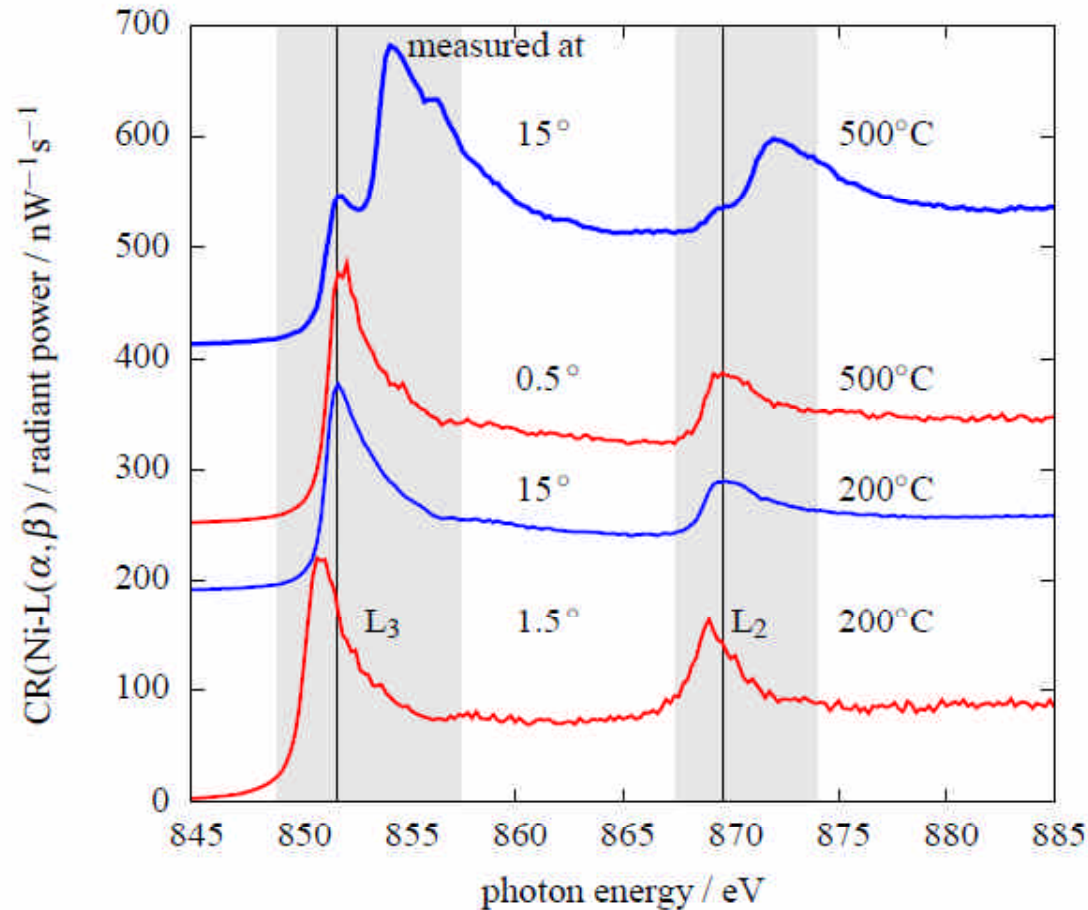


- Criterion: percentage of the maximum intensity
- Variation of the angle of incidence depending on the temperature for the interface analysis





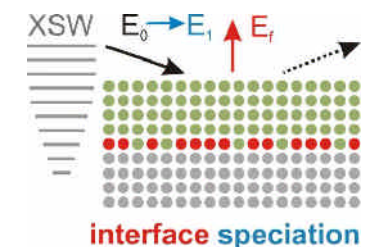
# Speciation of buried interfaces by GIXRF-NEXAFS



- **Comparison** between a **shallow** and a **steep** angle
- Interface observable: Ni-C, Ni-N or Ni-Si bonds possible

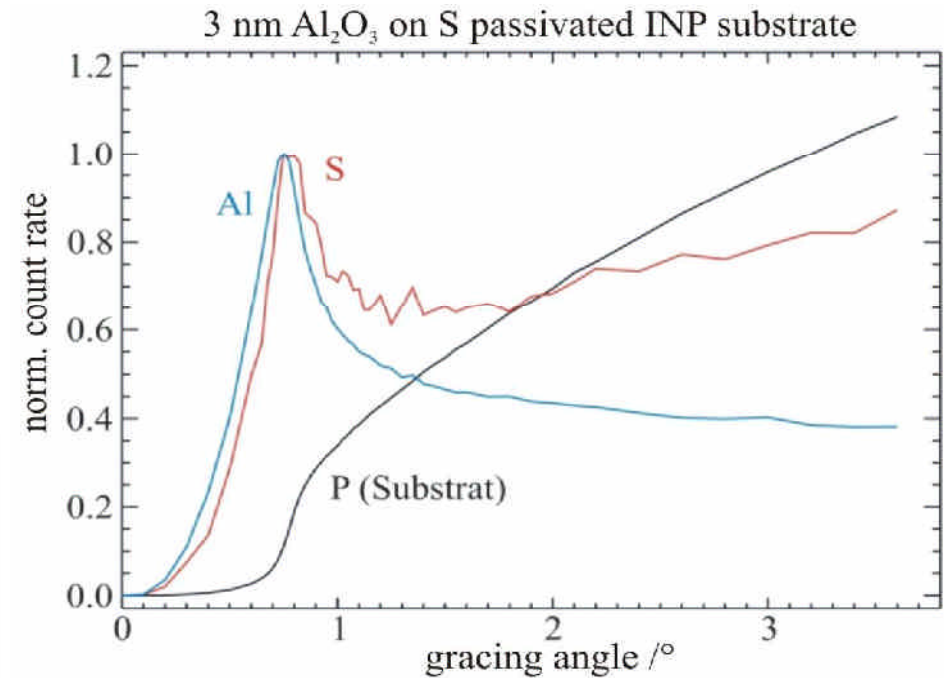
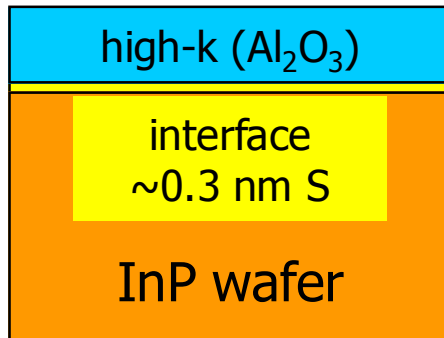
B. Pollakowski

Anal. Chem. **85**, 193 (2013)

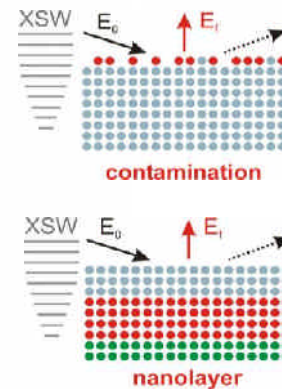
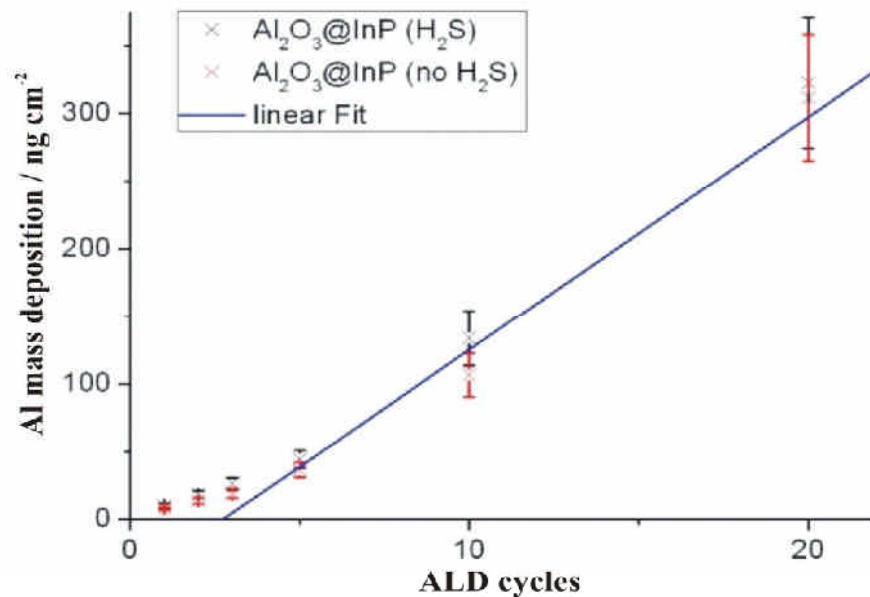


# Quantitative characterization of nanoelectronics

## Optimization of high-k nanolayer fabrication



## Quantification of the ALD growth rate

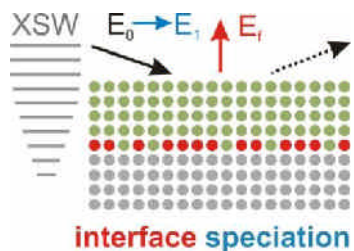
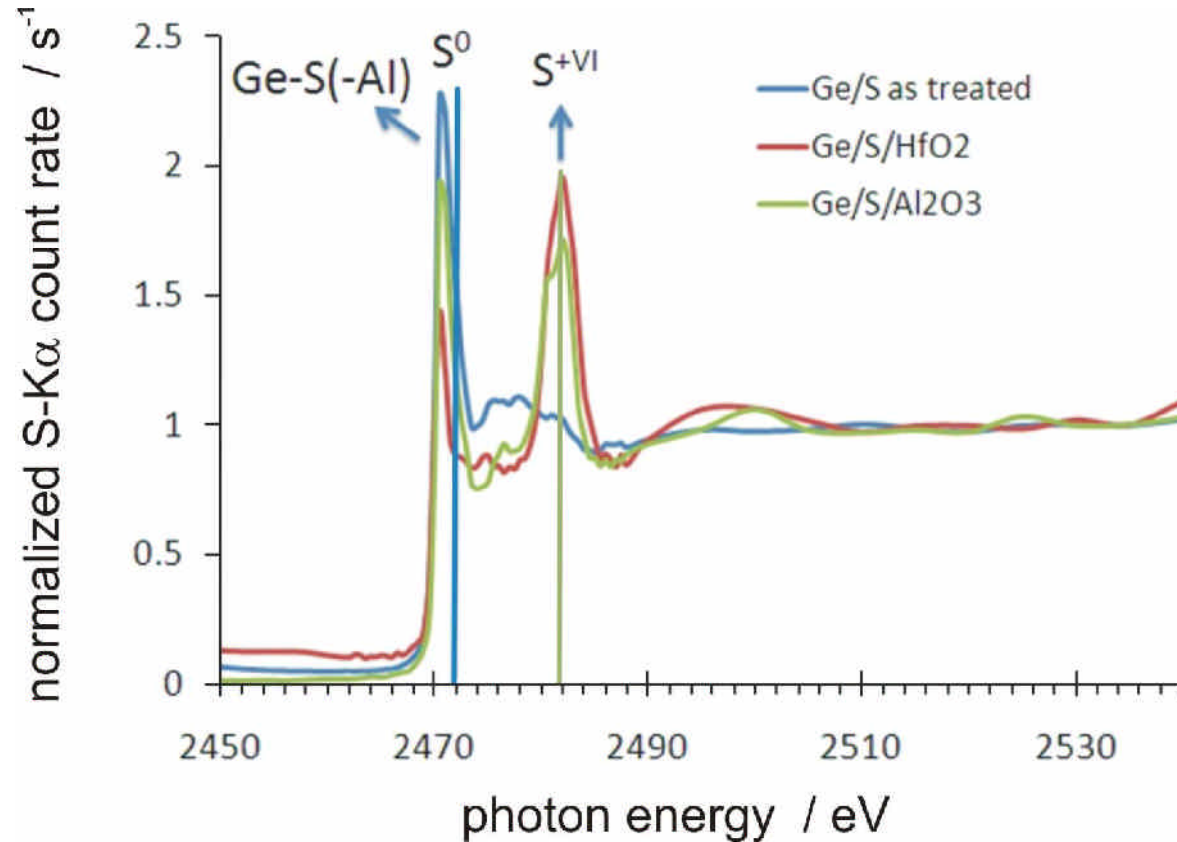


linear growth on S passivated InP substrate after the 3<sup>rd</sup> ALD cycle

J. Vac. Sci. Technol. A **30**, 01A127 (2012)

# Quantitative interface characterization and speciation

**XAFS speciation of the S passivated interface as treated and for two high k cap layer**



passivated interface  
(S monolayer ~0.3 nm)

M.Müller

J. Electrochem. Soc. **158**, H1090 (2011)



# GIXRF-NEXAFS at thin-film Si photovoltaics: probing the chemical state of buried interfaces

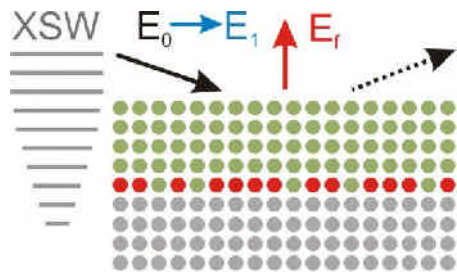
## GIXRF-NEXAFS requirements:

- transmission through a-Si layer
- total reflection at interface

Si:P - Si doped with 0,2 at% P

ZnO:Al - ca. 2 at.% Al

SiN - Si:N = 3:4

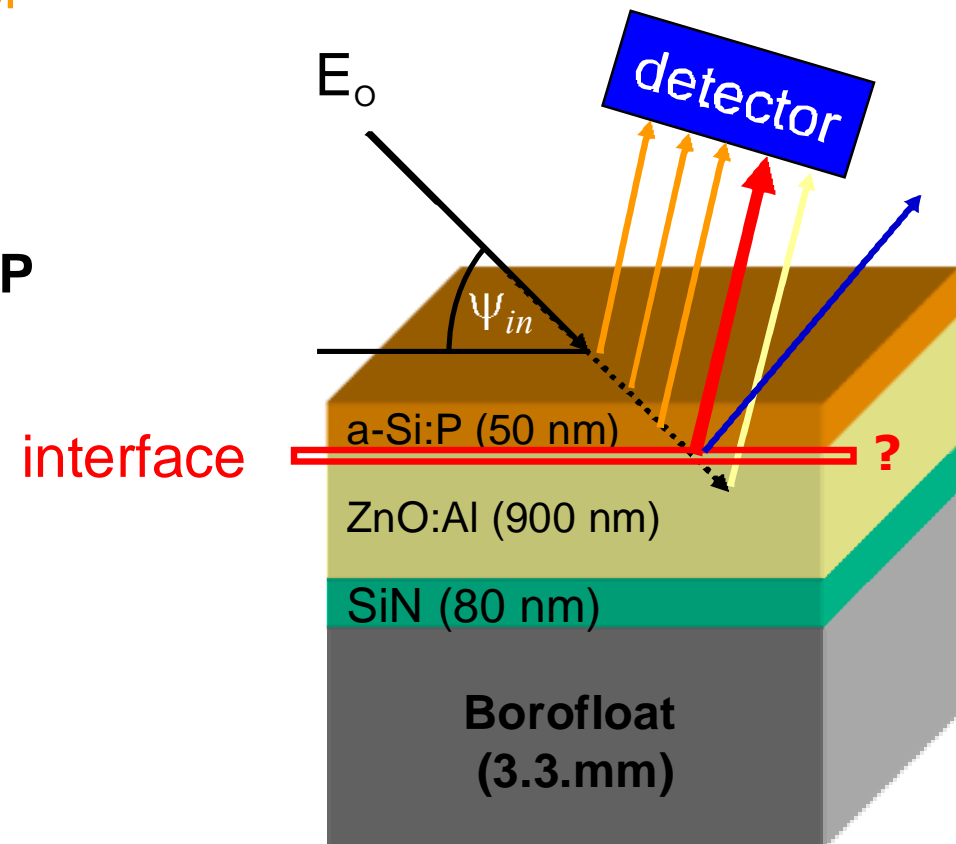


interface speciation

M. Pagels,  
TUB / HZB

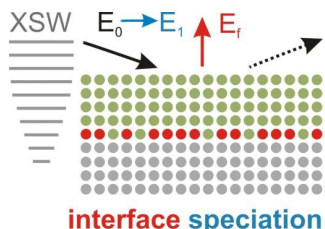
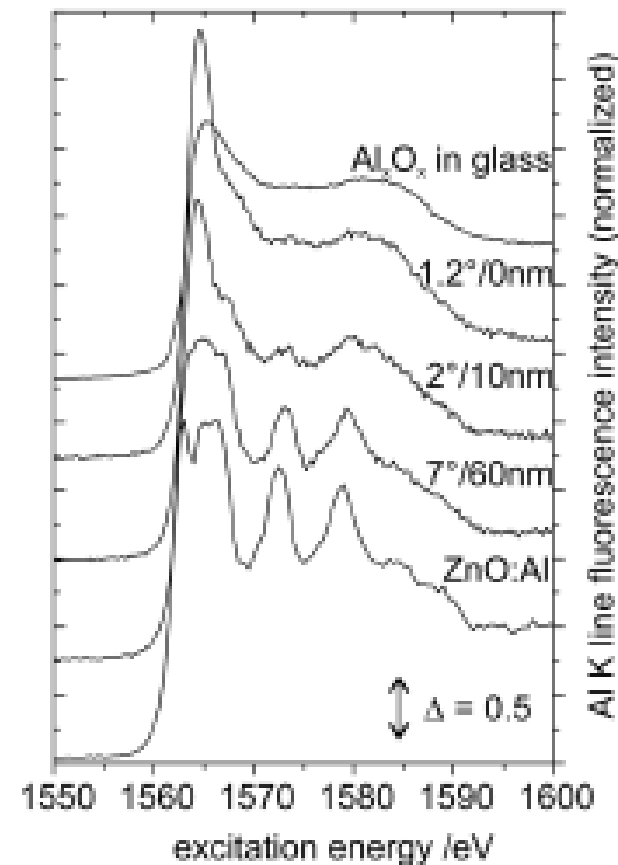
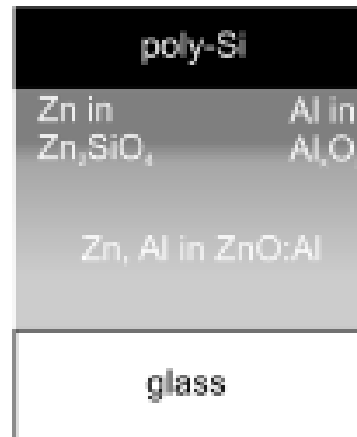
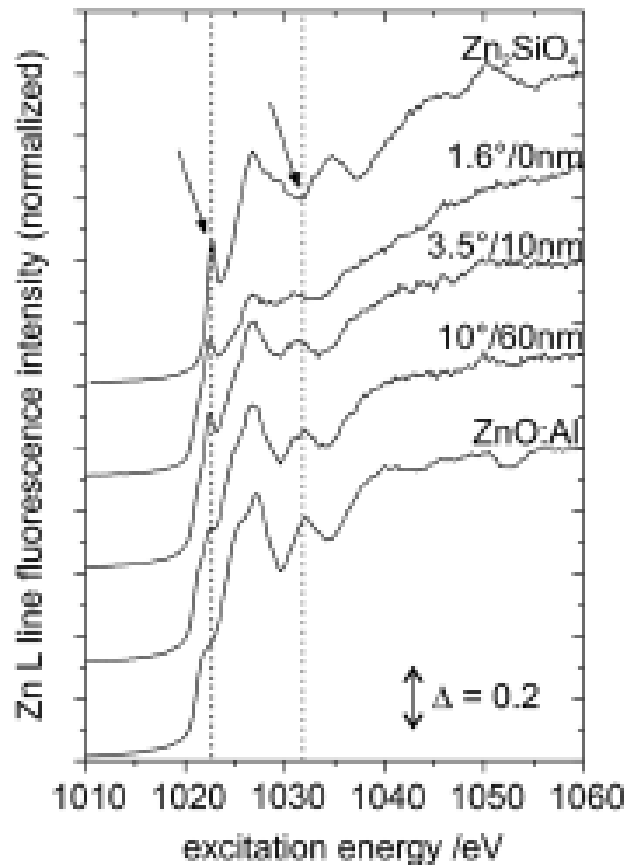
B. Pollakowski

NIMB 268, 370 (2010)



# GIXRF-NEXAFS at thin-film Si photovoltaics: probing the chemical state of buried interfaces

## NEXAFS investigations at the Zn-L<sub>iii,ii</sub> and Al-K edges



M. Pagels, TUB / HZB

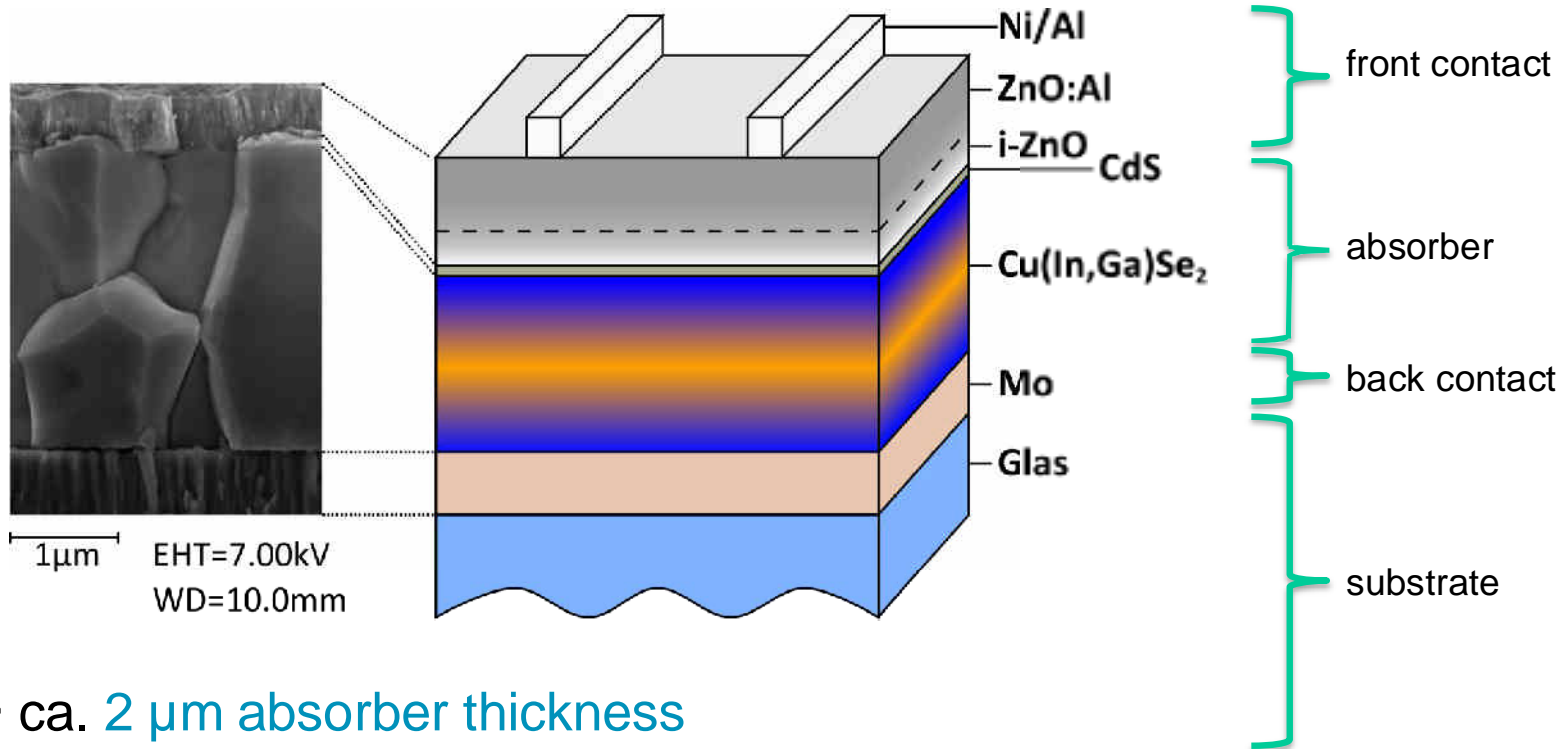
C. Becker, HZB

B. Pollakowski

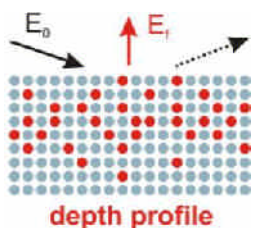
J. Appl. Phys. **113**, 044519 (2013)

# Elemental depth profiling of CIGS photovoltaics by GIXRF using calibrated instrumentation

## Cu(In,Ga)Se<sub>2</sub> absorber for thin film solar cells



- ca. 2 μm absorber thickness
- inhomogeneous element depth distribution of In and Ga influences the efficiency



# Elemental depth profiling of CIGS photovoltaics by GIXRF using calibrated instrumentation

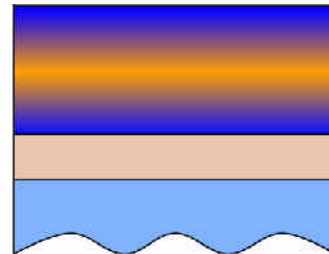


X-ray and IR spectrometry

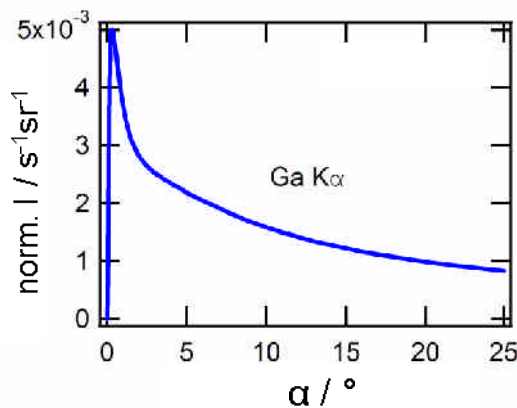
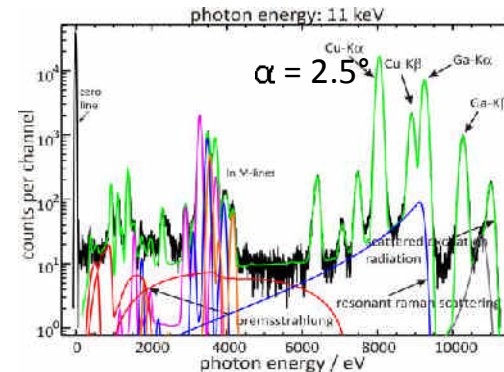


Increasing information depth with increasing incidence angle

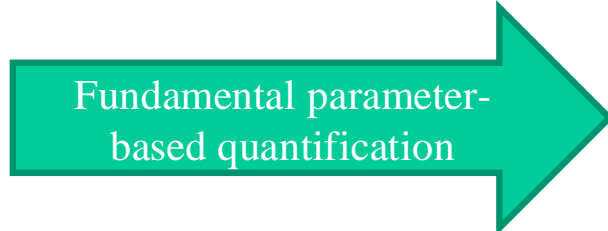
Fluorescence intensity in dependence of the angle of incidence



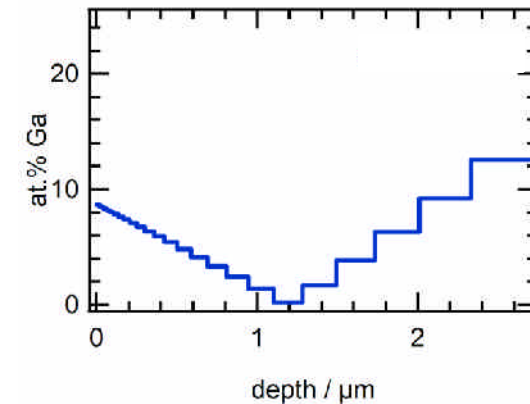
XRF-spectrum



Non-destructive access to the elemental depth profile



Elemental depth profile



# Comparison of in-depth resolving techniques

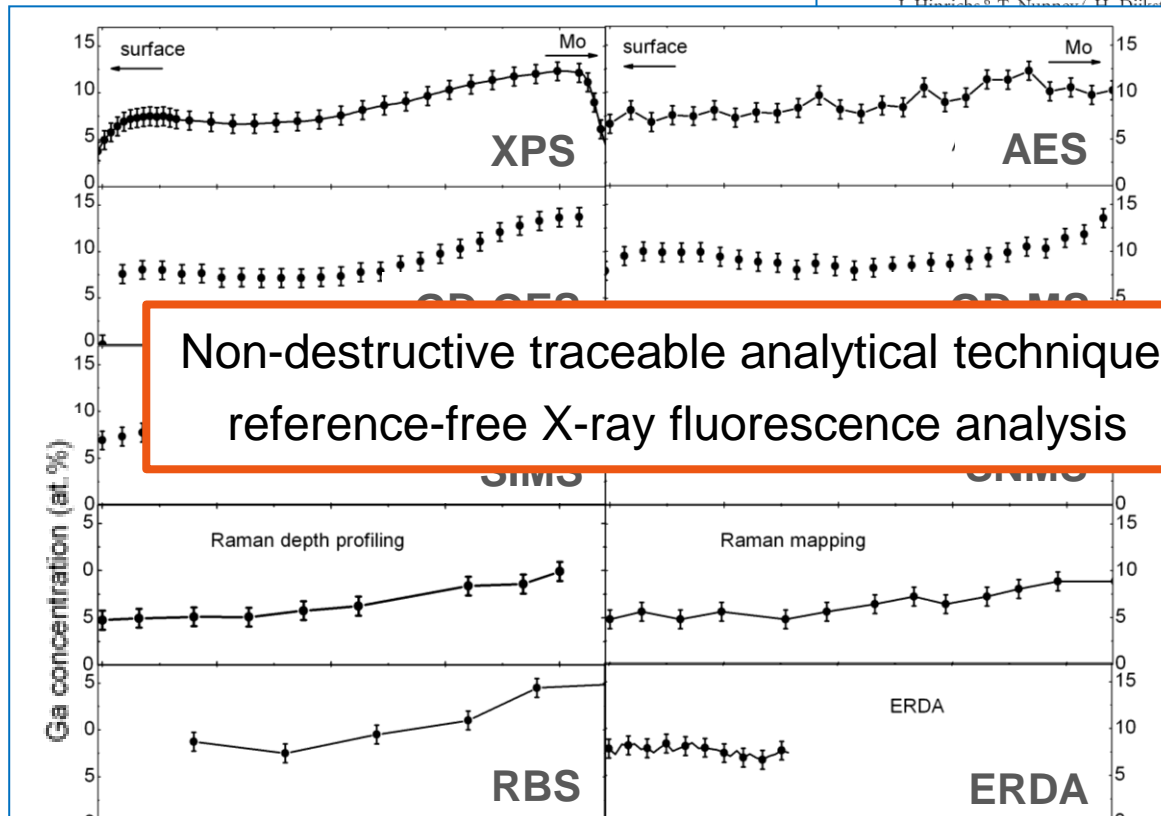
Microsc. Microanal. 17, 728–751, 2011  
doi:10.1017/S1431927611000523

Microscopy AND  
Microanalysis

© MICROSCOPY SOCIETY OF AMERICA 2011

## Comprehensive Comparison of Various Techniques for the Analysis of Elemental Distributions in Thin Films

D. Abou-Ras,<sup>1,\*</sup> R. Caballero,<sup>1</sup> C.-H. Fischer,<sup>1</sup> C.A. Kaufmann,<sup>1</sup> I. Lauer mann,<sup>1</sup> R. Mainz,<sup>1</sup> H. Mönig,<sup>1</sup> A. Schöpke,<sup>1</sup> C. Stephan,<sup>1</sup> C. Streeck,<sup>1</sup> S. Schorr,<sup>2</sup> A. Eicke,<sup>3</sup> M. Döbeli,<sup>4</sup> B. Gade,<sup>5</sup> J. Hirsch,<sup>6</sup> T. Nimmow,<sup>7</sup> H. Dülster,<sup>8</sup> V. Hoffmann,<sup>9</sup> D. Klemm,<sup>9</sup> V. Efimova,<sup>9</sup> A. Bergmaier,<sup>10</sup> A.A. Rockett,<sup>12</sup> A. Perez-Rodriguez,<sup>13,14</sup> J. Alvarez-Garcia,<sup>15</sup> P. Choi,<sup>17</sup> M. Müller,<sup>18</sup> F. Bertram,<sup>18</sup> J. Christen,<sup>18</sup> Ilac,<sup>19</sup> and I. Kötschau<sup>20</sup>



- more than 20 analytical techniques
- On sections of a laterally homogeneous sample
- Quantitative differences larger than uncertainties of single techniques
- Most methods require a calibration sample



# Elemental depth profiling of CIGS photovoltaics by GIXRF using calibrated instrumentation





X-ray and IR spectrometry

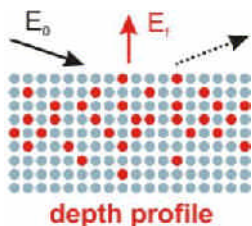
## Pilot-study CCQM-P140

### CCQM-P140

### SURFACE ANALYSIS

### Measurement of atomic fractions in Cu(In,Ga)Se<sub>2</sub> Films

Composition / at.%	Certified values  Korea Research Institute of Standards and Science	Reference-free GIXRF 
Cu	<b>23.8</b> ± 0.6	<b>24.0</b> ± 1.3
In	<b>19.1</b> ± 0.6	<b>19.3</b> ± 1.1
Ga	<b>6.6</b> ± 0.3	<b>6.3</b> ± 0.4
Se	<b>50.6</b> ± 1.5	<b>50.4</b> ± 2.8
d / μm	ca. <b>2</b>	<b>2.06</b> ± 0.09



C. Streeck

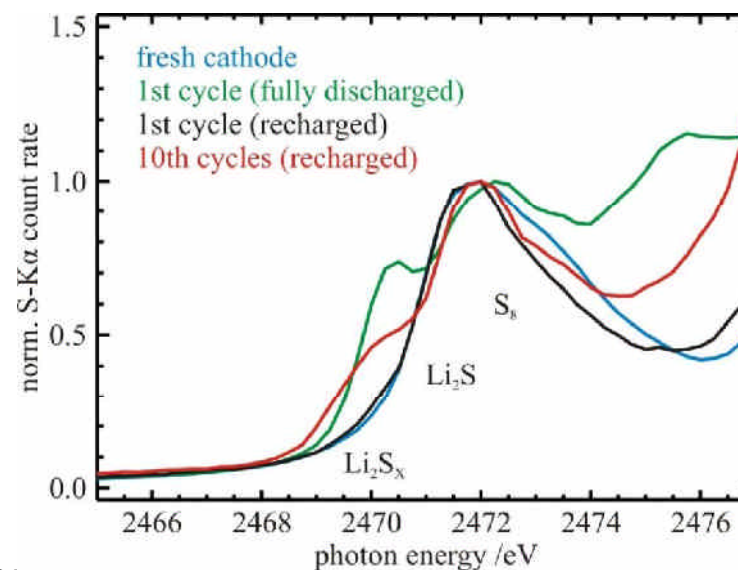
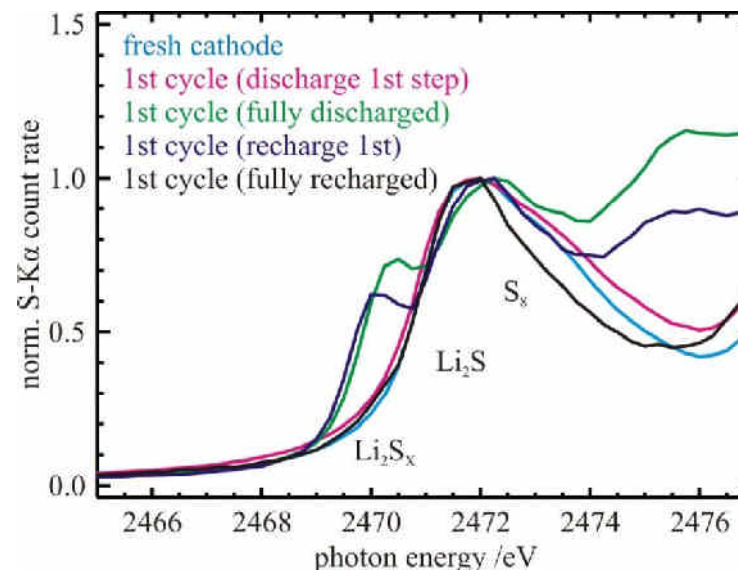
Metrologia, in print (2014)

# Directed development of new energy storage materials: towards in-operando XAFS speciation of cathode films

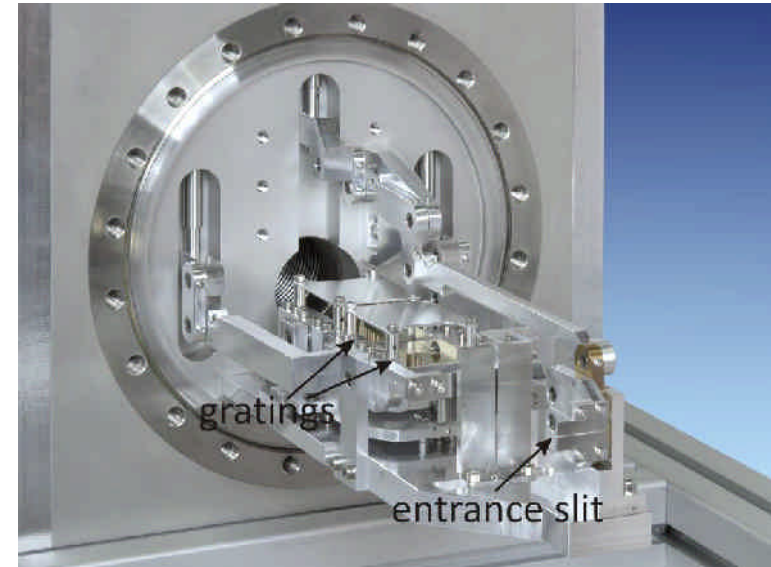
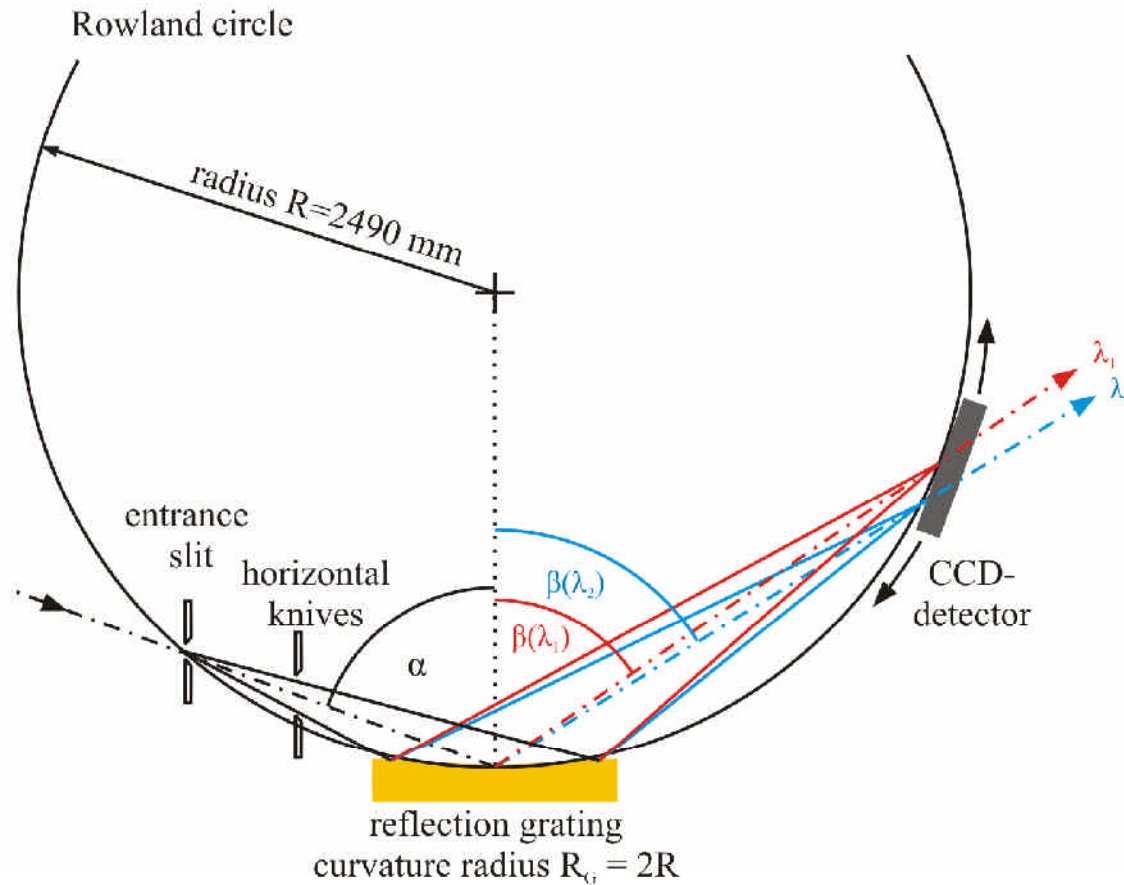
## First step: No ambient air exposure

Employing a thin window argon cell for transport and x-ray spectrometric measurements.

- NEXAFS measurements at different states of charge (not in-operando so far)
- Formation of lithium polysulfides during discharge observed
- Polysulfides disappear during recharge
- After several recharge cycles some of the polysulfides remain



# Calibrated Wavelength-Dispersive Spectrometer (WDS)

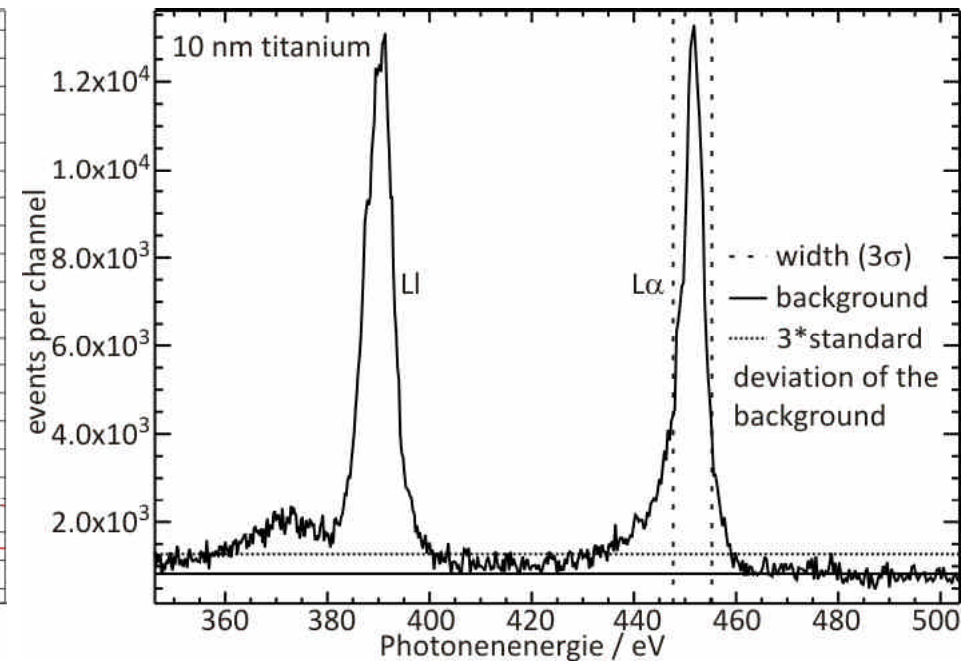
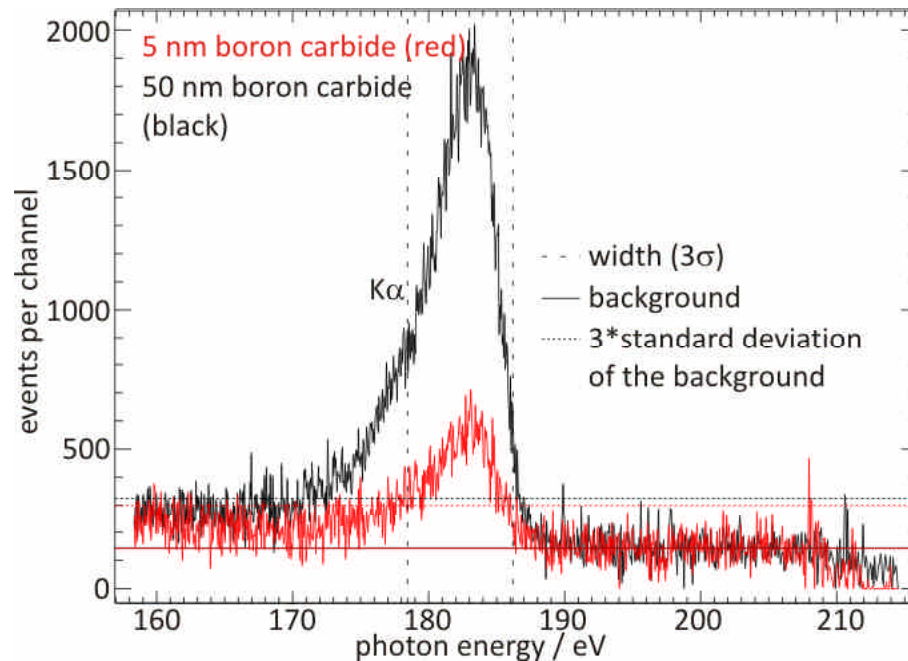


energy range:  
75 eV to 1760 eV  
energy resolution  $E/\Delta E$ :  
150 to 400

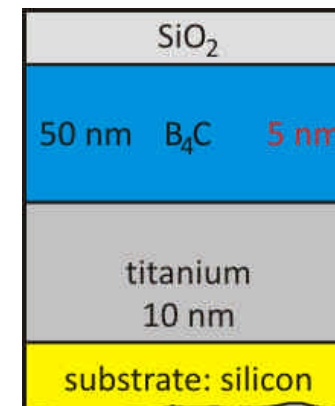
- calibration → allows for the determination of fundamental parameters
- disadvantage: → low efficiency, moderate detection limit, long integration time

# Calibrated Wavelength-Dispersive Spectrometer (WDS)

X-ray and IR spectrometry



- titanium (buried) measurable
- boron  $K\alpha$  (180 eV) detectable, despite a minimal sensitivity of the CCD
- lower limit of detection is in both cases (B and Ti) about 0.4 nm
- **access to thin films and buried nanolayers**



## Summary

---

- Reference-free analysis of contamination on Si and on novel materials
- Quantitative characterization of nanostructured and gradient systems ( $\sim 2 \mu\text{m}$ )
- Depth profiling ( $\sim 500 \text{ nm}$ ) and interfacial speciation of advanced materials
- Novel XRS instrumentation available at PTB, TUB, LNE-LNHB, IAEA/ELETTRA
- Calibrated high-resolution soft (and hard) x-ray emission spectrometer

[Further information](#) on reported activities and instrumentation

at **EMRP IND07** and **NEW01** at [www.EURAMET.org](http://www.EURAMET.org)



Acknowledgements: IMEC, KU Leuven, FhG IISB, LETI, LNHB, MEMC, Numonyx, Siltronic, Univ. Salford, HZB, IWS, AXO, FBK, KFKI AEKI, Technical Universities Berlin and Darmstadt, IPF

---

[ALTECH 2014 - 'Analytical techniques for precise characterization of nanomaterials'](#) symposium at the E-MRS spring meeting 2014 ( [www.european-mrs.com](http://www.european-mrs.com) ), France